Pontificia Universidad Católica del Perú

Escuela de Posgrado

Multi Domain Modelling of an Electromagnetic Fluid Valve and Sensitivity Analysis of Parameters of the Flux-Current Characteristic

Tesis para obtener el grado académico de Maestro en Ingeniería Mecatrónica que presenta:

Ing. Jorge Eduardo Gutiérrez Plasencia

Asesor PUCP (PUCP): *Prof. Dr. Ing. Julio César Tafur Sotelo*

Co-Asesor (no PUCP): *AOR PD Dr. -Ing. habil. Tom Ströhla*

Lima, 2025

Informe de Similitud

Yo, Julio César Tafur Sotelo, docente de la Escuela de Posgrado de la Pontificia Universidad Católica del Perú, asesor(a) de la tesis titulada(o) Multi Domain Modelling of an Electromagnetic Fluid Valve and Sensitivity Analysis of Parameters of the Flux-Current Characteristic, de el autor Jorge Eduardo Gutiérrez Plasencia, dejo constancia de lo siguiente:

- El mencionado documento tiene un índice de puntuación de similitud de 11%. Así lo consigna el reporte de similitud emitido por el software *Turnitin* el 30/09/2025.
- He revisado con detalle dicho reporte y la Tesis o Trabajo de investigación, y no se advierte indicios de plagio.
- Las citas a otros autores y sus respectivas referencias cumplen con las pautas académicas.

Lugar y fecha:

Lima, 30 de setiembre del 2025.

Apellidos y nombres del asesor / de la asesora: Tafur Sotelo, Julio Cesar	
DNI: 06470028	Firma 
ORCID: 0000-0003-3415-1969	

Selbständigkeitserklärung
Honour Statement

Ich erkläre hiermit, daß ich die vorliegende Arbeit selbständig verfaßt und keine anderen als die angegebenen Quellen benutzt habe. Alle Gedanken, die aus fremden Quellen direkt oder indirekt übernommenen wurden, sind als solche kenntlich gemacht. Die Arbeit wurde bisher keiner anderen Prüfungsbehörde vorgelegt und auch noch nicht veröffentlicht.

I hereby declare that I have written this thesis independently and have not used any other sources than those specified. All thoughts that have been taken either directly or indirectly from other sources have been explicitly identified as such. This thesis has not been submitted for credit in any other degree programme or institution nor has it been previously published.

Ilmenau, 15.07.2024

Ort, Datum | City, Date

Unterschrift | Signature

Resumen

El monitoreo de condiciones es un aspecto importante de muchas aplicaciones industriales estándares, y en los actuadores industriales modernos, en particular los actuadores de solenoide, sigue siendo un área de investigación activa. Esta tesis se centra en la válvula coaxial de la serie RSG 270, una válvula de fluido industrial del proyecto de investigación SmartValve. El objetivo principal es modelar el comportamiento magnético de la válvula utilizando el Método de Elementos Finitos (FEM) y simular tanto su comportamiento estático como transitorio. El estudio busca entender cómo los parámetros mecánicos influyen en la característica flujo-corriente (Ψ-i), ofreciendo así reducciones potenciales en el tiempo de ingeniería al minimizar la necesidad de realizar mediciones experimentales extensas en muestras de válvulas especialmente manipuladas.

La metodología incluye modelado 3D completo del circuito magnético del solenoide, simulaciones transitorias y estudios de parámetros. Las actividades clave incluyeron el cálculo de la distribución del flujo magnético en diversas condiciones operativas, el análisis de fuerzas transversales que actúan sobre un émbolo inclinado y la modelación 2D del circuito magnético para integrar la excitación eléctrica con parámetros mecánicos. Los estudios de parámetros examinaron factores como la posición inicial, la longitud del recorrido, la fricción, la rigidez del resorte de retorno y la temperatura. Las simulaciones se realizaron utilizando COMSOL Multiphysics, y los resultados fueron validados mediante la comparación con datos experimentales del proyecto SmartValve.

Los hallazgos clave incluyen ideas sobre la relación entre la corriente de excitación y el flujo magnético en condiciones transitorias, así como la sensibilidad del desempeño de la válvula ante variaciones en los parámetros mecánicos y eléctricos. Los resultados preliminares de simulación se alinearon estrechamente con los datos experimentales, demostrando un potencial significativo para el ahorro de tiempo y costos en el diseño y prueba de válvulas.

En conclusión, esta investigación contribuye a la comprensión de las válvulas electromagnéticas de fluidos al proporcionar un marco para modelar y analizar su comportamiento. Las contribuciones originales incluyen el modelado 3D del circuito magnético, la simulación transitoria de la relación flujo-corriente y un análisis básico de las fuerzas transversales en posiciones no coaxiales. Este trabajo sienta las bases para evaluar la viabilidad de implementar el monitoreo de condiciones en válvulas de solenoide.

Abstract

Condition monitoring is an important aspect of many standard industrial applications, and in modern industrial actuators, particularly solenoid actuators, it remains an area of active investigation. This thesis focuses on the RSG 270 series coaxial valve, an industrial fluid valve from the SmartValve research project. The primary objective is to model the magnetic behavior of the valve using the Finite Element Method (FEM) and to simulate both its static and transient behaviors. The study seeks to understand how mechanical parameters influence the flux-current characteristic (Ψ-i), offering potential reductions in engineering time by minimizing the need for extensive experimental measurements on specially manipulated valve samples.

The methodology includes comprehensive 3D modeling of the solenoid magnetic circuit, transient simulations, and parameter studies. Key activities involved calculating the magnetic flux distribution under various operating conditions, analyzing cross-forces acting on an inclined plunger, and performing 2D modeling of the magnetic circuit to integrate electrical excitation with mechanical parameters. Parameter studies examined factors such as initial position, stroke length, friction, return spring stiffness, and temperature. The simulations were carried out using COMSOL Multiphysics, and the results were validated by comparison with experimental data from the SmartValve project.

Key findings include insights into the relationship between excitation current and magnetic flux linkage under transient conditions, as well as the sensitivity of the valve's performance to variations in mechanical and electrical parameters. Preliminary simulation results closely aligned with experimental data, demonstrating significant potential for time and cost savings in valve design and testing.

In conclusion, this research contributes to the understanding of fluid electromagnetic valves by providing a framework for modeling and analyzing their behavior. Original contributions include 3D modeling of the magnetic circuit, transient simulation of the flux-current relationship, and a basic analysis of cross-forces in non-coaxial positions. This work lays the groundwork for the feasibility of implementing condition monitoring in solenoid valves.

Zusammenfassung

Die Zustandsüberwachung ist ein wichtiger Aspekt vieler standardisierter Industrieanwendungen und bleibt bei modernen Industrieaktuatoren, insbesondere bei Magnetaktuatoren, ein aktives Forschungsgebiet. Diese Arbeit konzentriert sich auf das koaxiale Ventil der Serie RSG 270, ein industrielles Fluidventil aus dem Forschungsprojekt SmartValve. Das Hauptziel ist die Modellierung des magnetischen Verhaltens des Ventils mithilfe der Finite-Elemente-Methode (FEM) sowie die Simulation seines statischen und transienten Verhaltens. Ziel der Studie ist es, zu verstehen, wie mechanische Parameter die Fluss-Strom-Kennlinie (Ψ-i) beeinflussen, und so mögliche Einsparungen in der Ingenieurszeit durch die Minimierung umfangreicher experimenteller Messungen an speziell manipulierten Ventilproben zu erzielen.

Die Methodik umfasst eine umfassende 3D-Modellierung des magnetischen Kreises des Magneten, transiente Simulationen und Parameterstudien. Zentrale Aktivitäten waren die Berechnung der magnetischen Flussverteilung unter verschiedenen Betriebsbedingungen, die Analyse der Querkräfte auf einen geneigten Anker sowie die Durchführung von 2D-Modellierungen des magnetischen Kreises zur Integration elektrischer Anregung mit mechanischen Parametern. Parameterstudien untersuchten Faktoren wie Anfangsposition, Hub, Reibung, Rückholfedersteifigkeit und Temperatur. Die Simulationen wurden mit COMSOL Multiphysics durchgeführt, und die Ergebnisse wurden durch Vergleich mit experimentellen Daten aus dem SmartValve-Projekt validiert.

Wesentliche Erkenntnisse umfassen Einblicke in die Beziehung zwischen Erregerstrom und magnetischem Fluss bei transienten Bedingungen sowie die Empfindlichkeit der Ventilleistung gegenüber Variationen mechanischer und elektrischer Parameter. Erste Simulationsergebnisse stimmten eng mit experimentellen Daten überein und zeigen ein erhebliches Potenzial für Zeit- und Kosteneinsparungen bei der Ventilauslegung und -prüfung.

Zusammenfassend trägt diese Forschung zum Verständnis von elektromagnetischen Fluidventilen bei, indem ein Rahmen für die Modellierung und Analyse ihres Verhaltens bereitgestellt wird. Originalbeiträge umfassen die 3D-Modellierung des magnetischen Kreises, die transiente Simulation der Fluss-Strom-Beziehung und eine grundlegende Analyse der Querkräfte in nicht-koaxialen Positionen. Diese Arbeit bildet die Grundlage für die Machbarkeitsprüfung der Zustandsüberwachung bei Magnetventilen.

Contents

Nomenclature

Variable	Description	Unit
B_z	Magnetic field intensity	T
F_x	Force component in x-direction	N
F_y	Force component in y-direction	N
F_z	Force component in z-direction	N
F_r	Friction force	N
F_{k0}	Spring preload	N
I_p	Current applied to coil	A
k	Return spring stiffness	N/mm
m_{vAn}	Average slope of Ψ vs I curve	$\frac{\text{Wb}}{\text{A}\cdot\text{mm}}$
Ψ	Magnetic flux linkage	Wb
Ψ_{diff}	Difference in concatenated flux Ψ	Wb
Ψ_{start}	Initial flux at start of movement	Wb
S_p	Cross-sectional area of piston	m^2
T	Temperature	°C
T_{max}	Maximum temperature for analysis	°C
Δt	Time interval	s
d_{gap}	Initial air gap between piston and core	mm
N	Number of turns in coil	-
v_I	Rate of change of current	A/s
v_z	Velocity in axial direction	mm/s
x, z, z_p	Piston position	mm
δ_{min}	Minimum residual air gap	mm

Acronym	Description
AC	Alternate Current
AI	Artificial Intelligence
B-H	Magnetic Flux Density (B) vs. Magnetic Field Strength (H)
Ψ-i	Flux-Current Characteristic
DAE	Differential-Algebraic Equation
FEA	Finite Element Analysis
FEM	Finite Element Method
MMF	Magnetomotive Force
ODE	Ordinary Differential Equation

1 Introduction

Condition monitoring is an important aspect of electric actuators, such as servomotor-driven systems and solenoids, which are widely used in modern industrial applications for their precision and reliability [1]. Solenoid actuators, which consist of a coil of electrical wire and an armature, act as electromagneto-mechanical energy converters. Their performance can be characterized by measuring voltage, current, and evaluating magnetic field effects [2]. However, while condition monitoring has been extensively studied in servomotor-driven systems, solenoid actuators have received comparatively less attention in this regard. Understanding their behavior under various operating conditions remains an area of ongoing research.

This thesis investigates an industrial fluid valve from the SmartValve research project, focusing on modeling its magnetic behavior using the Finite Element Method (FEM) and simulating both static and transient behaviors. The study aims to bridge the knowledge gap by elucidating how mechanical parameters influence the flux-current (Ψ-i) characteristic, which is critical for optimizing performance and reliability. Unlike previous studies that relied heavily on experimental measurements, this work leverages advanced simulation techniques to reduce engineering time and cost [3].

Electromagnetic valves are devices that convert electromagnetic energy into mechanical motion to control the flow of fluids. They are integral to numerous industrial applications where performance and reliability are paramount. Existing research has provided valuable insights into the basic functioning of these valves. However, a detailed understanding of how mechanical and electrical parameter variations impact their behavior is still lacking. For instance, studies often focus on specific operational conditions without exploring the interplay of multiple parameters in a comprehensive manner. This thesis addresses this limitation by developing robust models that simulate the valve's behavior under a range of conditions, thereby offering a more holistic

understanding.

The primary contributions of this work include the development of 3D and 2D FEM models to simulate static and transient behaviors, detailed parameter studies, and validation against experimental data. These contributions advance the state of the art by demonstrating the feasibility of accurate simulations as a substitute for extensive physical testing. Moreover, the findings provide actionable insights for optimizing valve design and operational strategies, thereby enhancing reliability and efficiency [4].

1.1 Objectives

The primary objectives of this research are:

- To develop 3D and 2D FEM models of an industrial fluid valve for simulating static and transient behaviors.
- To investigate the effects of mechanical parameters, such as initial position, stroke, friction, return spring stiffness, and temperature, on the valve's performance.
- To validate simulation results against experimental data from the SmartValve project, ensuring model accuracy and reliability.
- To propose a simulation-based methodology that reduces dependency on extensive experimental measurements.

1.2 Methodology

The methodology of this research involves the following steps:

- Using COMSOL Multiphysics for FEM simulations to model the electromagnetic and mechanical behavior of the valve.
- Employing SOLIDWORKS for designing and refining the valve's geometry.
- Analyzing simulation data using MATLAB R2024a to extract performance metrics and validate results.

- Conducting parameter studies to evaluate the influence of key mechanical and electrical parameters on valve performance.
- Comparing simulation outcomes with existing experimental measurements to ensure alignment and accuracy.

1.3 Scope

The scope of this study includes:

- Electromagnetic and mechanical modeling of an industrial fluid valve using FEM.
- Development of both 3D and 2D models for comprehensive analysis.
- Investigation of static and transient behaviors under varying operational conditions.
- Analysis of mechanical parameters such as stroke, friction, and temperature effects on valve performance.

Limitations:

- Reliance on simulation tools and the accuracy of models to represent real-world conditions.
- Experimental validation limited to comparisons with existing measurements; physical prototyping and testing of new valve designs are outside the scope of this work.

1.4 Thesis Outline

This thesis is organized as follows:

- Chapter 1: Introduction. Presents the background, objectives, methodology, scope, and outline of the thesis.
- Chapter 2: State of the Art. Reviews relevant literature on electromagnetic valve modeling and simulation techniques.
- Chapter 3: Computational Modeling and Analysis Methodology. Details the development

of FEM models and simulation setup.

- Chapter 4: Parameter Studies and Sensitivity Analysis. Explores the influence of key parameters on valve performance.
- Chapter 5: Conclusions and Future Work. Summarizes key findings and proposes directions for future research.

2 State of the Art

2.1 Fundamental Concepts of Electromagnetic Actuators

2.1.1 Classification of Electromagnets

Electromagnets encompass a diverse array of designs and configurations, each tailored to specific applications within engineering and technology. Understanding their classification based on structural design, geometric shape, and magnetic properties is fundamental for selecting the most suitable type for a given task.

Structurally, they can be classified based on their design and construction. Solenoids represent one common category, consisting of a coil wound around a core. They find extensive use in applications requiring linear motion or the generation of magnetic fields. Relays, another structural classification, serve the purpose of controlling the flow of electrical current. They typically comprise coils, armatures, and contacts, facilitating the switching of electrical circuits. Linear actuators transform electrical energy into linear motion, making them essential in robotics, industrial machinery, and automotive systems. Similarly, rotary actuators convert electrical energy into rotary motion, enabling precise positioning in various mechanical systems. Beyond these general categories, specialized configurations of electromagnets exist to address specific application requirements, such as disk-shaped or hybrid designs [4].

Solenoids, a common type of electromagnet, are widely used in applications requiring linear motion or the generation of magnetic fields. They consist of a coil wound around a core. Figures 2.1a and 2.1b illustrate the model of a solenoid actuator and the forces applied to the mover, respectively.

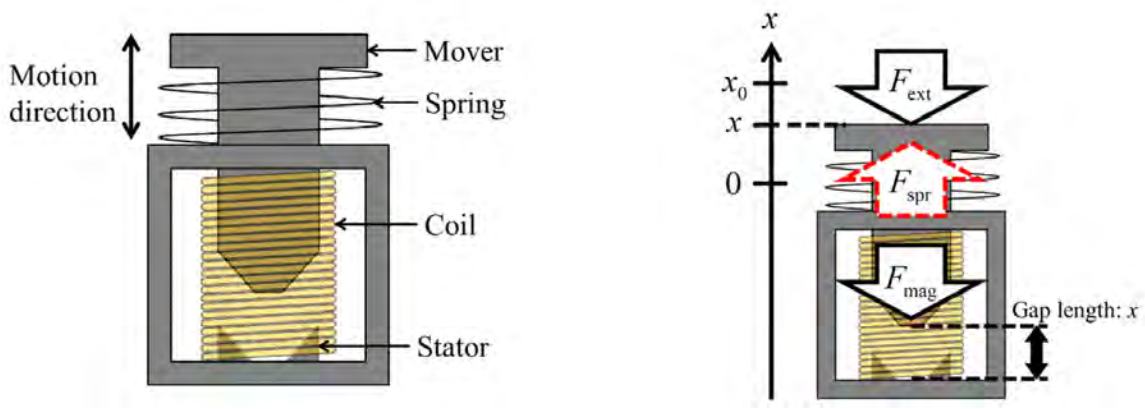

(a) Model of a solenoid actuator.

(b) Forces applied to the armature.

Figure 2.1: Solenoid actuator modeling and forces [5].

Geometric classification offers another perspective, categorizing electromagnets based on their physical shape and form factor. Cylindrical electromagnets, for instance, are commonly found in solenoids and linear actuators. They feature a cylindrical core around which the coil is wound, providing a compact and efficient design for generating magnetic fields or inducing linear motion. Tubular electromagnets are similar, but exhibit a hollow core structure that allows for the insertion of rods or shafts. This configuration is often employed in applications requiring extended travel or actuation distances. Disk-shaped electromagnets possess a flat and circular geometry, making them particularly suitable for rotary actuators where rotational motion is desired. Additionally, custom shapes of electromagnets, such as E and U-shaped configurations, are engineered to meet specific spatial constraints or functional requirements, offering flexibility in design and application [4] (see Figure 2.2).

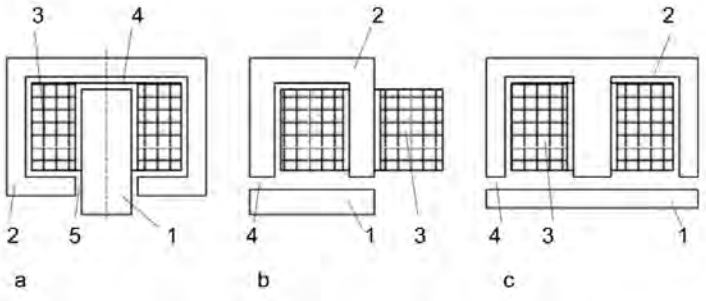

Figure 2.2: Basic forms of electromagnets: (a) pot magnet, (b) U-magnet, (c) E-magnet. 1: armature, 2: stator, 3: excitation coil, 4: working air gap, 5: parasitic air gap [4].

Magnetic property-based classification considers the materials and magnetization mechanisms employed in electromagnet construction. Permanent magnet electromagnets utilize perma-

nent magnets, which retain their magnetic properties without the need for an external power source. These electromagnets offer advantages such as increased holding force and energy efficiency, making them suitable for applications requiring sustained magnetic fields. Soft magnetic material-based electromagnets rely on materials like iron or steel with high permeability to enhance magnetic flux density and improve performance. They are commonly used in electromechanical devices where rapid changes in magnetic fields are required, such as transformers and inductors. Polarized electromagnets combine electromagnetic coils with permanent magnets or soft magnetic materials to leverage the benefits of both approaches, achieving a balance between efficiency, holding force, and versatility [4].

In the context of sensorless actuation systems, solenoid actuators are particularly noteworthy due to their compact size and high efficiency. These systems can significantly reduce the overall size and complexity of applications, especially where precise motion control is required without the addition of physical sensors [5]. Solenoid actuators find extensive use in valves, switches, and braking systems, emphasizing their importance across various engineering fields.

2.1.2 Static and Dynamic Behaviour of Electromagnets

Electromagnets exhibit both static and dynamic behaviours, each essential for understanding their operation and applications.

- **Static Behaviour**

  In electromagnetics, static behaviour refers to the characteristics of the electromagnet under steady-state conditions, where variables such as current, magnetic field, and force remain constant. One crucial aspect of static behaviour is the attraction force analysis, which involves determining the force exerted by the electromagnet on nearby ferromagnetic objects. This analysis relies on calculating the magnetic flux density distribution within the core material and evaluating the resulting force based on material properties and geometric factors [6].

  Another key consideration in static behaviour analysis is magnetic reluctance calculation. Magnetic reluctance quantifies the opposition to magnetic flux within a material or magnetic circuit and plays a significant role in determining the efficiency of magnetic flux

transmission. By assessing the reluctance of the magnetic circuit comprising the electromagnet's core and surrounding materials, engineers can optimize the design for improved performance and energy efficiency [6].

Additionally, inductance measurement is vital for characterizing the static behaviour of electromagnets. Inductance provides insights into the electrical properties and performance characteristics of the electromagnet's coil winding. By measuring inductance in various configurations and operating conditions, engineers can determine factors such as coil impedance, self-inductance, and mutual inductance, essential for designing efficient electromagnetic circuits and optimizing control strategies [7].

In Figure 2.3, a diagram of the magnetic field of a simplified electromagnet is shown, illustrating the field lines.

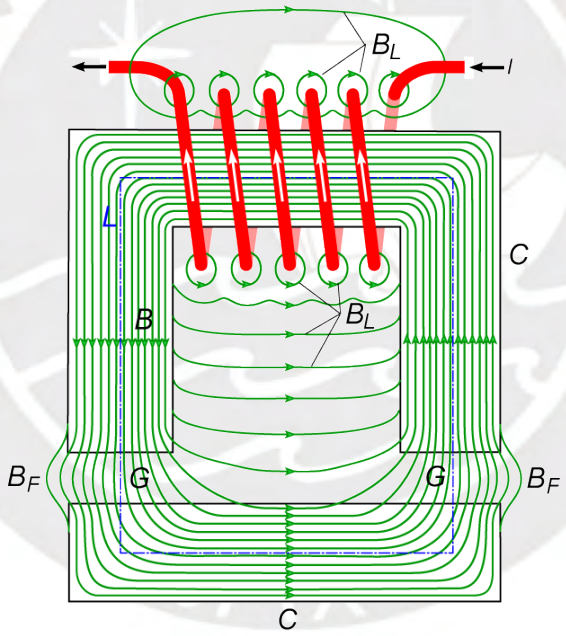

Figure 2.3: Diagram of the flux lines of a typical electromagnet (adapted from Chetvorno, 2010, Wikimedia Commons).

- **Dynamic Behaviour**

  This analysis focuses on how electromagnets respond to changes in operating conditions, such as variations in excitation current and mechanical loads. Understanding the dynamic response is crucial for designing responsive and adaptive electromechanical systems.

  One aspect of dynamic behaviour is the electromagnet's response to changes in excitation

current. Variations in excitation current, resulting from control signals or system disturbances, affect the electromagnet's magnetic field strength and attraction force. Analyzing this response helps engineers design electromechanical systems with precise control and optimal performance [6]. Recent studies have demonstrated the use of current and voltage signal analysis for diagnosing faults in electromechanical devices, highlighting the importance of understanding dynamic behaviour for effective fault diagnosis [8].

Moreover, electromagnets exhibit dynamic responses to mechanical load variations, such as changes in position, velocity, or acceleration of connected components. Studying how electromagnets respond to these loads provides insights into their force-displacement characteristics, response time, and energy consumption. This understanding is critical for designing electromechanical systems that meet performance requirements, such as precision positioning and rapid actuation [8].

For instance, analyzing the current and flux linkage trends over time can provide valuable information on the electromagnet's performance and potential fault conditions. Figure 2.4 illustrates an example of a normalized current–flux linkage curve, showing both the current and flux linkage trend with respect to time and a two-dimensional plot between current and flux linkage.

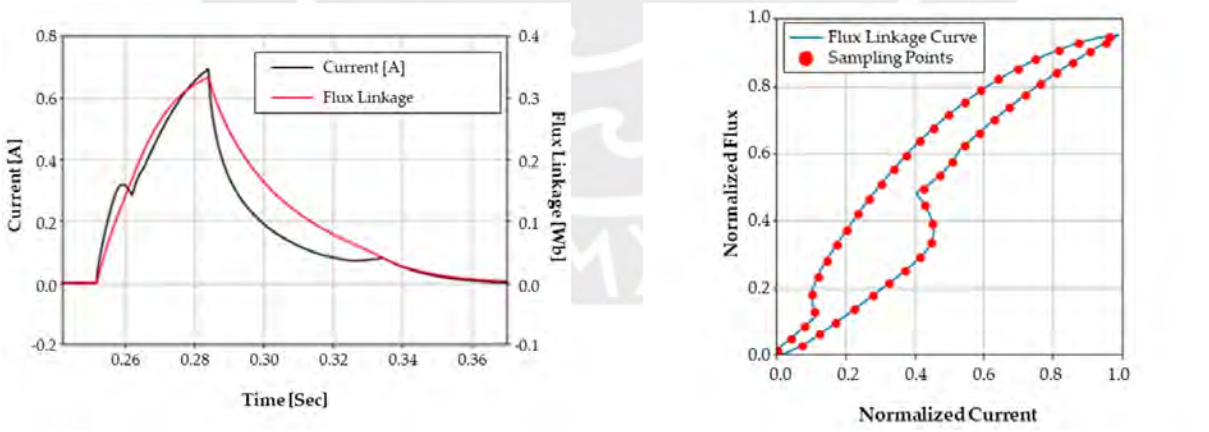

(a) Current and flux linkage trend with respect to time.

(b) Two-dimensional plot between current and flux linkage.

Figure 2.4: An example of a normalized current–flux linkage curve [8].

According to Kallenbach et al. [4], the dynamic behaviour of electromagnets can be described using a set of differential equations that represent the electrical, magnetic, mechanical, and thermal aspects. The simplified basic structure of the electromagnet as a

dynamic energy converter is shown in Figure 2.5.

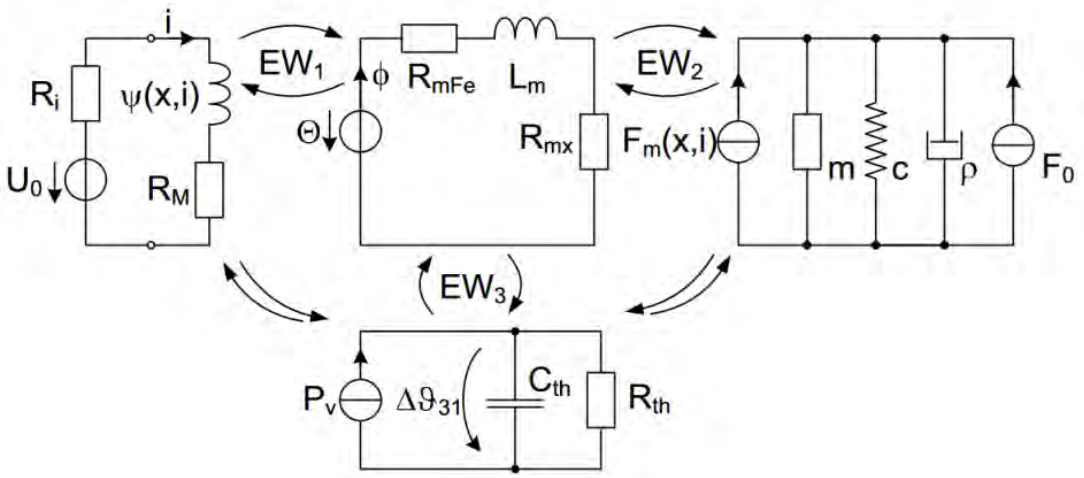

Figure 2.5: Simplified basic structure of the electromagnet as a dynamic energy converter [4].

The key equations that describe the dynamic behaviour, encompassing the electrical, magnetic, mechanical, and thermal aspects, are as follows:

$$U_0 = i \cdot (R_i + R_M) + \frac{d\Psi(x,i)}{dt} \tag{2.1}$$

$$\Theta = \Phi \cdot (R_{mFe} + R_{mx}) + L_m \cdot \frac{d\Phi}{dt} \tag{2.2}$$

$$F_m(x,i) = m\ddot{x} + \rho\dot{x} + cx + F_0 \tag{2.3}$$

$$P_v = C_{th} \cdot \frac{d\Delta\vartheta_{31}}{dt} + \frac{\Delta\vartheta_{31}}{R_{th}} \tag{2.4}$$

Where:

- U_0 is the voltage provided by the power source.
- i is the current through the electromagnet.
- R_i and R_M are the resistances of the power source and the coil, respectively.
- $\Psi(x,i)$ is the magnetic flux linkage as a function of position x and current i.

- Θ is the magnetomotive force (MMF).
- Φ is the magnetic flux.
- R_{mFe} and R_{mx} are the magnetic resistances of the iron core and the air gap, respectively.
- L_m is the magnetic inductance.
- $F_m(x, i)$ is the magnetic force as a function of position x and current i.
- m is the mass of the armature.
- ρ is the damping coefficient.
- c is the spring constant.
- F_0 is the pre-load force of the spring.
- P_v is the power loss in dissipative components.
- C_{th} is the thermal capacitance.
- $\Delta\vartheta_{31}$ is the temperature difference between the environment and the electromagnet.
- R_{th} is the thermal resistance.

These equations describe the interaction between electrical input, magnetic field generation, mechanical movement, and thermal effects within an electromagnet. Understanding these interactions is essential for predicting the dynamic performance and optimizing the design of electromechanical systems.

Electromagnets exhibit both static and dynamic behaviours, each essential for understanding their operation and applications. In this context, it's crucial to note that in simulations using COMSOL, we analyze key variables such as excitation current I, plunger position x, magnetic force on the plunger F, and magnetic flux linkage Ψ. Here, I and x serve as input variables, while F and Ψ are dependent variables. This theoretical framework enables us to investigate and establish relationships among these variables through numerical simulations.

During steady-state data acquisition ($\frac{d\Phi}{dt} = 0$), and considering $\Theta = N \cdot I$, we reshape

the equation 2.2:

$$N \cdot I = \Phi \cdot (R_{mFe} + R_{mx}) \tag{2.5}$$

where R_{mFe} is constant, and R_{mx} depends on the position x of the plunger. Rearranging gives:

$$\Phi = \frac{N \cdot I}{R_{mFe} + R_{mx}} \tag{2.6}$$

resulting in the function $\Psi = f_1(I, x)$. Note that in the COMSOL simulations, z was used to represent position, while x is used in this thesis.

Furthermore, the magnetic force F on the plunger is directly related to the magnetic flux linkage Ψ through the magnetic circuit. According to Ampère's law:

$$\oint \mathbf{H} \cdot d\mathbf{l} = I_{enc} \tag{2.7}$$

where $\mathbf{H}$ is the magnetic field intensity, $d\mathbf{l}$ is a differential element of length along the closed loop, and I_{enc} is the current enclosed.

For an inductor, the relationship between the magnetic flux Ψ and the magnetic field intensity $\mathbf{H}$ is given by:

$$\Psi = \frac{B \cdot A}{\mu} \tag{2.8}$$

where B is the magnetic flux density, A is the cross-sectional area, and μ is the magnetic permeability.

The magnetic force F on the plunger is related to the gradient of the magnetic energy W stored in the inductor:

$$W = \frac{1}{2} L \Psi^2 \tag{2.9}$$

where L is the inductance of the system.

Thus, the magnetic force F can be expressed as:

$$F = \frac{dW}{dx} = L\Psi\frac{d\Psi}{dx} \tag{2.10}$$

Under appropriate symmetry and magnetic field distribution conditions, it is established that: $F \propto \Psi^2$.

Consequently, in this model, F is also a function of the variables I and x, denoted as $F = f_2(I, x)$, highlighting the dependence of the electromagnetic force on both the coil excitation current I and the plunger position x.

This theoretical framework not only facilitates the investigation of relationships among these variables but also validates the model through numerical simulations in COMSOL, where I and x are treated as input variables and F and Ψ as dependent variables.

2.1.3 Measurement of Magnetic Properties and Ψ(i, δ) Characteristic

Understanding the magnetic quantities and relations of electromagnets is crucial for their efficient design and performance optimization. In the context of simulating electromagnetic valves, precise measurement of these properties plays a pivotal role in developing accurate simulation models that replicate real-world behaviors. By integrating experimental data from magnetic property measurements into simulation frameworks, engineers can enhance the predictive accuracy of these models, ensuring that simulated outcomes closely reflect actual valve performance under varying operating conditions.

- **Magnetic Property Measurement**

  Measuring the magnetic properties of electromagnets involves quantifying parameters such as magnetic flux density, magnetic field strength, and permeability. These measurements provide insights into the electromagnet's ability to generate magnetic fields and interact with ferromagnetic materials.

  One common method for measuring these properties is using magnetic field sensors such as Hall effect sensors or fluxgate magnetometers [9]. These sensors detect the strength

and direction of magnetic fields produced by the electromagnet, allowing for precise measurements crucial in electromagnet design and analysis. Additionally, field measurement coils and magnetic voltage meters are often used for applications requiring precise field measurements [4].

For more precise measurements, techniques such as vibrating sample magnetometry (VSM) and superconducting quantum interference device (SQUID) magnetometry are employed. These methods are particularly useful for characterizing the magnetic behavior of materials used in electromagnet construction, such as iron cores or magnetic alloys [4, 9].

Yang et al. [10] highlight the importance of measuring magnetic properties such as hysteresis and core loss distributions. Additionally, Jiles [9] provides comprehensive coverage of the principles and methodologies for accurately measuring magnetic properties, detailing the significance of parameters like magnetic susceptibility, permeability, and hysteresis loops.

Xu et al. [11] introduce a novel vectorial elemental operator model to analyze magnetic hysteresis in soft magnetic composite (SMC) materials under diverse magnetization conditions. Their approach offers valuable insights into the complex magnetic behaviors of SMC materials, which are crucial for advancing electromagnetic device design.

- Φ**(i,** δ**) Characteristic Analysis**

  The Φ(i, δ) characteristic, also known as the flux linkage or magnetic flux linkage, describes the relationship between the electromagnet's magnetic flux and its excitation current and displacement. Analyzing this characteristic curve provides valuable insights into the electromagnet's performance, particularly in relation to force production and energy storage potential.

  Characterizing the Φ(i, δ) curve involves measuring the electromagnet's magnetic flux linkage at various excitation current levels and displacements. This data is then plotted to generate the characteristic curve, which typically exhibits nonlinear behaviour due to magnetic saturation effects and mechanical constraints [8].

  The shape of the Φ(i, δ) curve is influenced by the magnetic properties of the core ma-

terial, as described by its B-H curve. The B-H curve illustrates the relationship between magnetic flux density (B) and magnetic field strength (H), capturing phenomena such as magnetic saturation and hysteresis. Understanding how changes in excitation current and displacement affect the Φ(i, δ) curve is crucial for optimizing electromagnet design and performance [8].

Analyzing the Φ(i, δ) characteristic allows engineers to determine key parameters such as magnetic saturation limits, hysteresis effects, and operating regions where the electromagnet exhibits optimal performance. This information is useful for designing control strategies that maximize force output while minimizing energy consumption and ensuring stable operation under varying load conditions [8].

In this context, Kallenbach et al. [4] describe the $\Psi(i, \delta)$ characteristic analysis method, which involves measuring the induced back EMF in the excitation coil. The excitation coil itself is used as the sensing element, eliminating the need for a secondary coil for voltage measurement, as shown in Figure 2.6. This method allows for the assessment of integrated actuators without modifications.

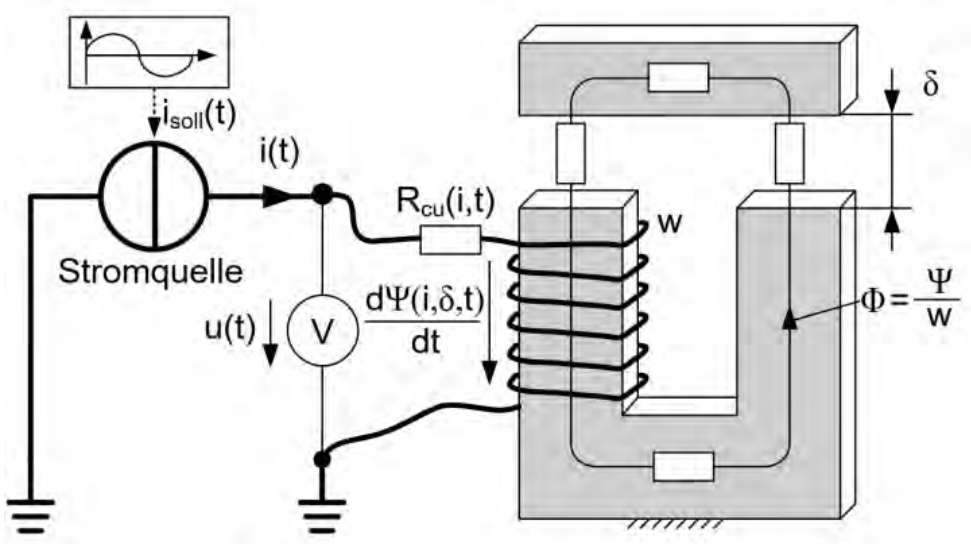

Figure 2.6: $\Psi(i, \delta)$ characteristic measurement setup (Stromquelle: current source) [4].

Figure 2.7 illustrates the Ψ-I characteristic curve of the coaxial valve, adapted from [3]. This curve showcases the relationship between induced voltage (Ψ) and current (I), crucial for understanding the performance under different operating conditions.

The lower hysteresis curve segment corresponds to the connection process, while the

upper segment corresponds to disconnection. The middle portion of the curve (in blue) results from the movement of the armature.

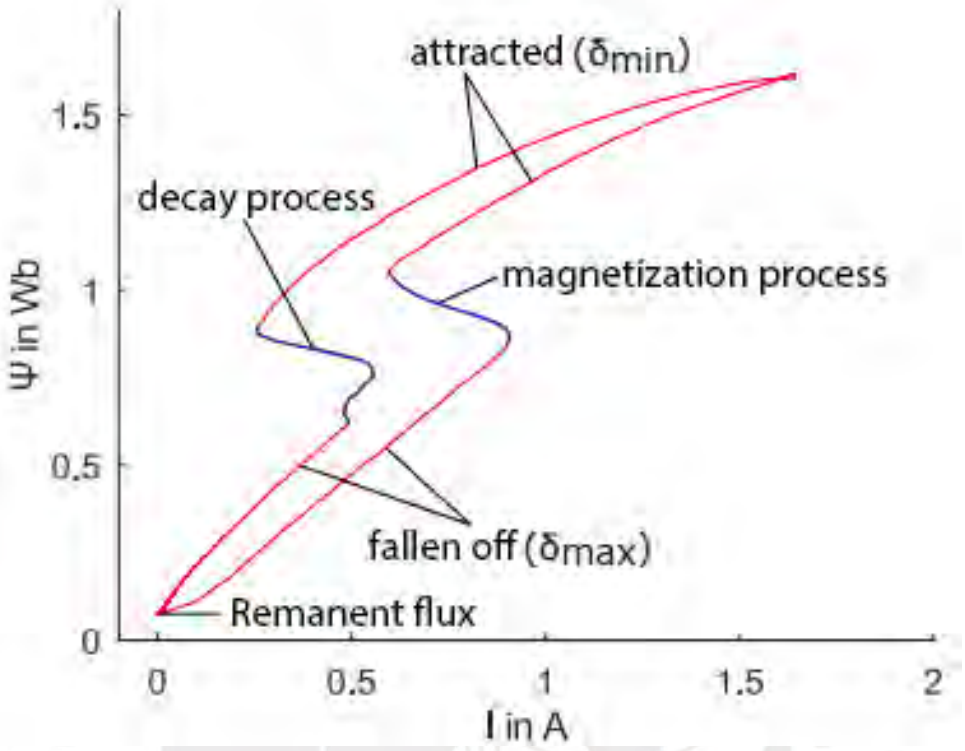

Figure 2.7: $\Psi(i, \delta)$ characteristic curve illustrating startup and shutdown processes. Adapted from [3].

The $\Psi(i, \delta)$ characteristic provides a comprehensive evaluation of the electromagnetic-to-mechanical energy conversion in the actuator. Comparing the measured $\Psi(i, \delta)$ characteristic of a test part with that of a known good part can determine if the test part meets the required specifications. Furthermore, monitoring the $\Psi(i, \delta)$ characteristic over the actuator's lifespan can help detect wear and changes in mechanical properties that affect magnetic energy conversion [4].

2.1.4 Description of Considered Electromagnetic Valves

Electromagnetic valves play a vital role in various engineering systems, particularly in fluid control applications where precise regulation of flow is required. Understanding their classification, internal structure, and signs of wear and failure is essential for effective design, maintenance, and troubleshooting.

- **Classification Based on Design**

  Electromagnetic valves can be classified based on their design characteristics, which include factors such as the number of ports, valve type (e.g., spool, poppet), actuation mechanism (e.g., direct-acting, pilot-operated), and arrangement. One notable type is the coaxial valve, characterized by its concentric design, where the fluid flow path is aligned along a common axis. Coaxial valves are commonly used in applications requiring compact design and minimal fluid turbulence.

  This classification helps engineers select the most suitable valve configuration for specific applications, considering factors such as flow rate requirements, pressure conditions, and fluid compatibility [12].

  Common classifications include two-way and three-way valves, normally open and normally closed valves, and direct-acting and pilot-operated valves [12]. Each type offers unique advantages and limitations, influencing factors such as response time, power consumption, and reliability .

  As illustrated in Figure 2.8, the schematic diagrams depict the principle and operation of a direct-operated 2/2-way coaxial valve, adapted from [13].

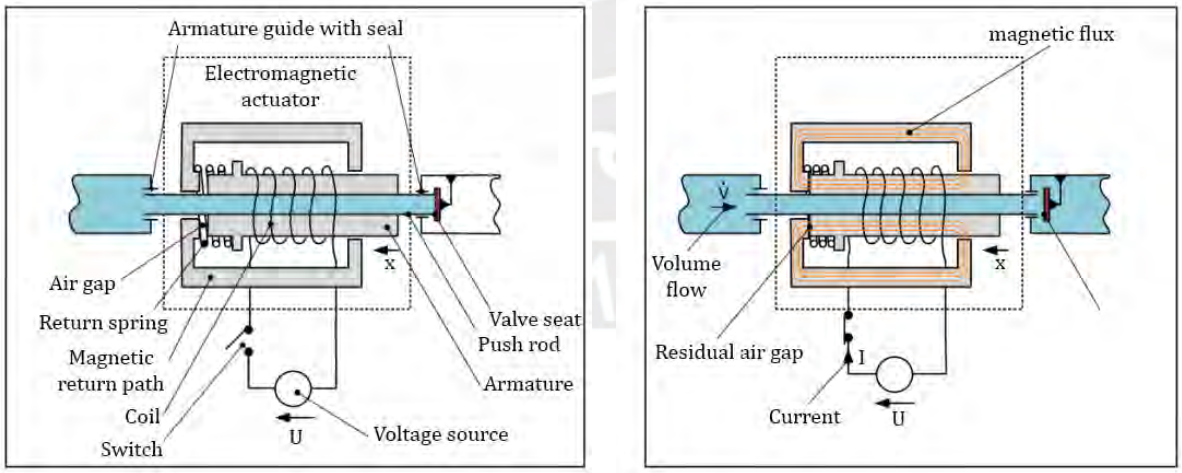

(a) De-energized state (valve closed).

(b) Energized state (valve open).

Figure 2.8: Schematic diagrams of a direct-operated 2/2-way coaxial valve, with labels translated from German to English, adapted from [13].

- **Structure and Components**

  The internal structure of electromagnetic valves typically consists of essential compo-

nents such as a solenoid coil, armature, plunger, valve seat, and fluid passages. The solenoid coil generates a magnetic field when energized, attracting the armature and causing the plunger to move, thereby opening or closing the valve. The valve seat provides a sealing surface to control fluid flow, while the fluid passages direct the flow path within the valve assembly.

Understanding the structure and function of these components is crucial for designing and optimizing electromagnetic valves for specific applications. Factors such as material selection, component dimensions, and assembly tolerances influence valve performance, durability, and reliability.

As shown in Figure 2.9, the cross-sectional view of a directly controlled coaxial valve from the 270 DN15 series provides a detailed illustration of its components. This is the electromagnetic valve that will be simulated for this thesis.

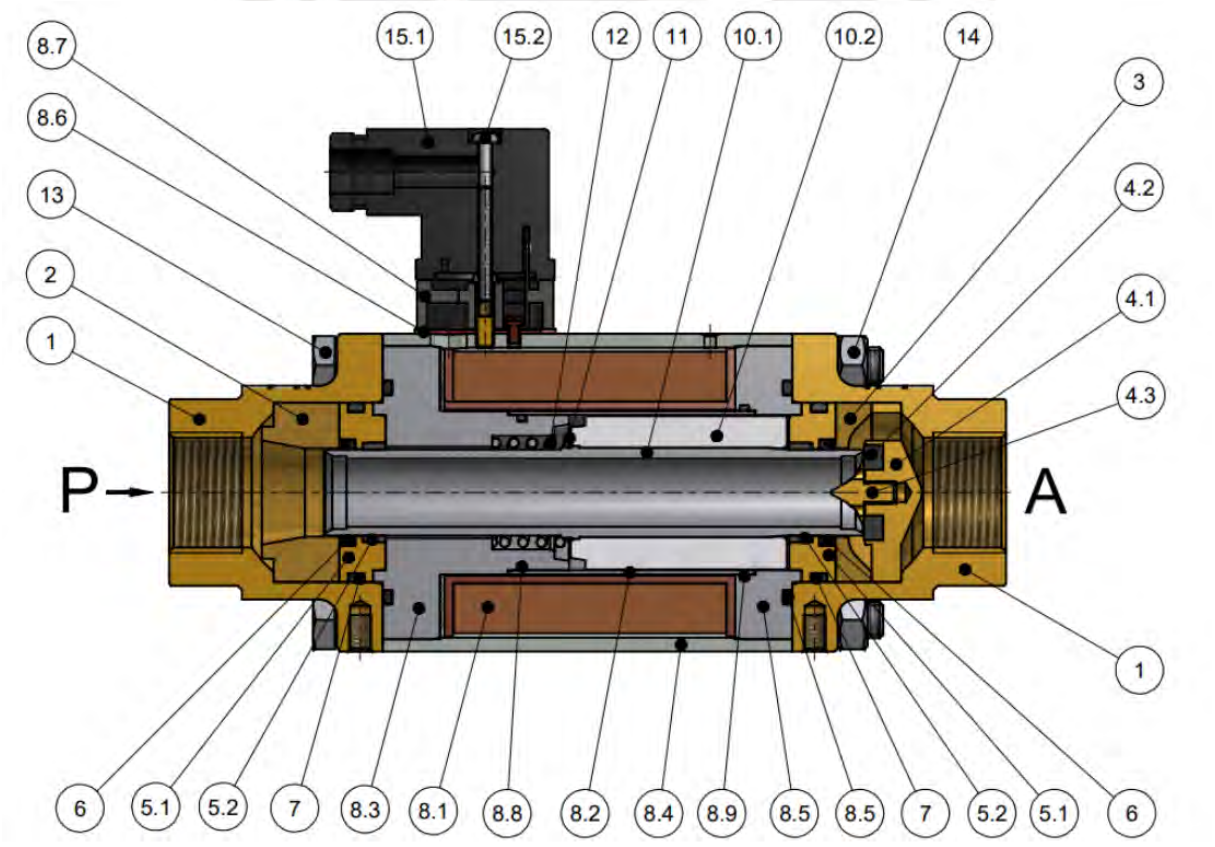

Figure 2.9: Cross-sectional view of a directly controlled coaxial valve from the 270 DN15 series, adapted from [13].

As detailed in Table 2.1, the main components of the directly controlled coaxial valve

from the 270 DN15 series are listed below.

Table 2.1: Components of the Directly Controlled Coaxial Valve Series 270 DN15 according to [13]

Pos.	Description	Pos.	Description	Pos.	Description
1	Connection piece	7	O-Ring 34.59x2.62	9	O-Ring 42.52x2.62
2	Spacer	8	Electromagnetic drive (coil)	10	Electromagnetic drive (armature or control tube)
3	Cover	8.1	Copper coil	10.1	Plunger tube (control tube)
4	Valve seat	8.2	Guide tube	10.2	Plunger sleeve (armature)
4.1	Valve seat raw part	8.3	Magnetic core	11	Anti-remanence disk
4.2	Vulcanized elastomer seal	8.4	Coil housing	12	Compression spring (return spring)
4.3	Valve seat cone	8.5	Magnetic cover	13	Hexagon bolt M8x120
5	Guide disk	8.6	Flat gasket	14	Hexagon nut M8
5.1	Guide disk	8.7	Radius connector	15	Device socket
5.2	Guide bushing	8.8	O-Ring 31x1.5	15.1	Device socket
6	Dynamic seal	8.9	O-Ring 36x1.5	15.2	Screw M3x35

- **Signs of Wear and Failure**

  Like any mechanical device, electromagnetic valves are subject to wear and potential failure over time, particularly in demanding operating conditions or due to inadequate maintenance. Common signs of wear and impending failure include leakage, erratic valve operation, reduced flow capacity, and increased power consumption.

  Identifying these signs early through regular inspection and monitoring allows for timely maintenance or replacement, minimizing downtime and preventing costly system failures.

  As discussed in [13], the dynamic seals (position number 6), valve seat seals (position number 4.2), and guide bushings (position number 5.2) are particularly prone to wear. Additionally, for water as the medium, deposits on the plunger tube and armature (position numbers 10.1 and 10.2) and corrosion can occur.

2.2 Modelling of Electromagnetic Valves

This section explores the fundamental aspects of creating mathematical and computational representations of electromagnetic valves to predict their behaviour under various operating conditions. It covers analytical modelling, finite element analysis, dynamic simulation, and model validation.

2.2.1 Analytical Modelling

This approach begins with simplifying the physical system into a set of equations that describe the relationships between electrical, magnetic, and mechanical parameters. These models are typically based on fundamental principles of electromagnetism and mechanics. By assuming linearity and ignoring higher-order effects, analytical models can provide quick and reasonably accurate predictions of valve behaviour. They are useful for initial design stages and for gaining insights into the primary factors affecting valve performance. Analytical models often include parameters such as coil inductance, magnetic reluctance, and mechanical spring constants, allowing engineers to derive expressions for force, displacement, and response times.

In this context, Peng et al. [14] provide a comprehensive study on the analysis and identification of a dynamic model for a proportional solenoid. Their work highlights the importance of simplified mathematical models to capture the static and dynamic characteristics of the solenoid, which can be beneficial for engineers and technicians in the initial design and performance evaluation stages.

Additionally, in this thesis, the analytical modelling serves as a basis for understanding the behaviour of the electromagnetic valve using the theory mentioned in Subchapter 2.1.2.

2.2.2 Finite Element Analysis

FEA is a powerful computational tool used to model electromagnetic valves with high precision. It involves discretising the valve geometry into small finite elements and solving Maxwell's equations numerically for each element. This method can accurately account for complex geometries, nonlinear material properties, and intricate boundary conditions. FEA allows for de-

tailed analysis of the magnetic field distribution, eddy currents, and mechanical stresses within the valve, simulating transient behaviour and identifying areas of magnetic saturation to optimise coil designs and improve overall valve performance.

Likewise, Xiao-qing and Long [15] enhance analysis efficiency and accuracy by combining magnetic circuit analysis with FEA, fitting FEM results with algebraic equations for use in analytical and simulation software.

Similarly, Guo et al. [16] optimized the magnetic isolation ring position in AC solenoid valves to improve dynamic response, demonstrating the impact of precise modelling and simulation. An example of geometry discretisation of a valve is shown in Figure 2.10.

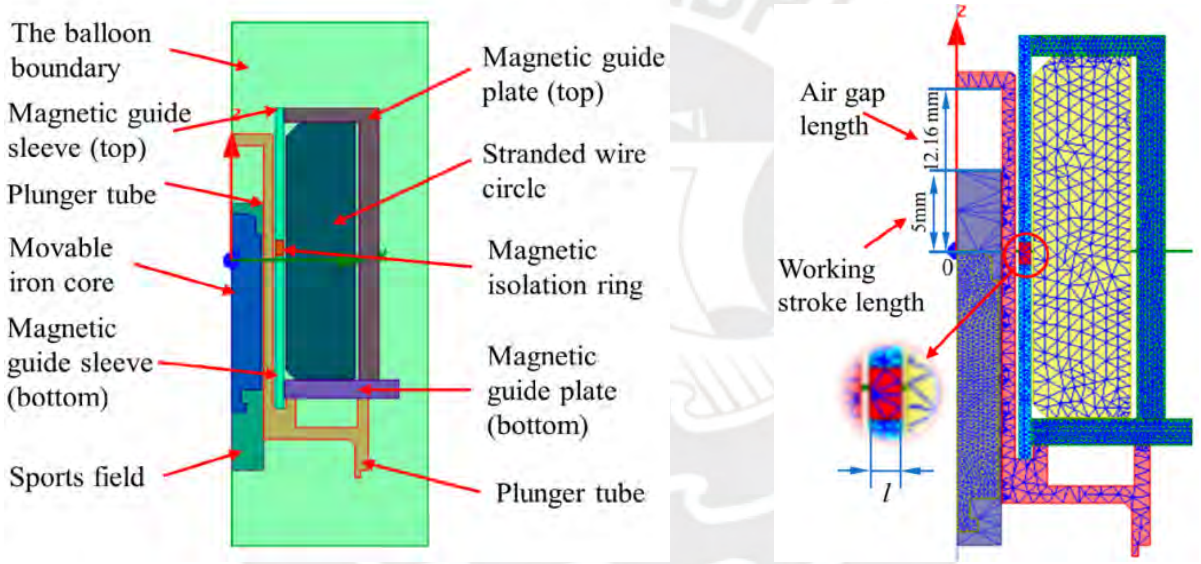

(a) Solution settings

(b) Meshing the magnetic conductive material

Figure 2.10: An example of geometry discretisation of a valve [16].

2.2.3 Dynamic Simulation

This technique involves modelling the time-dependent behaviour of electromagnetic valves. This includes simulating how the valve responds to changes in electrical input, such as varying current or voltage, and how it interacts with mechanical loads. Dynamic models typically involve coupling electromagnetic equations with mechanical motion equations, necessitating the solution of a set of differential equations [17]. These simulations can capture transient phenomena like coil energisation, magnetic force build-up, and valve movement. They are essential

for designing control systems, as they provide insights into the response time, stability, and robustness of the valve under different operating conditions.

Furthermore, Assi [18] demonstrated the importance of dynamic simulation in the design and validation of an electromagnet for a time-varying magnetic flux leakage system, highlighting how simulations can differentiate between defects in nondestructive testing applications.

2.2.4 Model Verification

Validating the accuracy of finite element models involves comparing the simulation results with findings from other established FEM studies. This process helps in verifying the reliability of the developed models by ensuring consistency with previously published research. Discrepancies between different studies are analysed to identify potential areas for model improvement [18]. Effective comparison with existing FEM studies instils confidence in using these models for design optimisation and performance evaluation of electromagnetic valves.

For instance, Meng et al. [19] demonstrated the importance of validating models through comparisons between measured and simulated current in the coil of an electromagnetic valve under standard operating conditions (24-volt input).

2.3 Finite Element Method (FEM) in Electromagnetic Modelling

Finite Element Method (FEM) is a powerful numerical technique widely used in engineering and physics to solve complex problems involving differential equations. The fundamental principles of FEM involve discretizing a certain volume into much smaller, simpler parts called finite elements. These elements are connected at nodes, and the equations governing the behaviour of the system are approximated over these elements. One of the primary advantages of FEM is its versatility; it can handle complex geometries, material properties, and boundary conditions with relative ease [20]. However, FEM also has limitations, such as high computational costs and the need for substantial knowledge in setting up and interpreting models, unlike the requirements for circuit models. In electromagnetic systems, FEM is particularly valuable

for analysing and designing components where precise control of magnetic fields and forces is critical.

In the context of electromagnetic actuators, FEM analysis involves several key steps. Mesh generation is the process of dividing the domain into finite elements, and it is crucial for the accuracy and efficiency of the simulation [20]. A well-defined mesh captures the geometry and physical behaviour of the system accurately. Material property assignment follows, where each element is assigned properties such as permeability, conductivity, and magnetization characteristics. Accurate representation of these properties is essential for realistic simulations. Boundary conditions must also be applied to define how the system interacts with its environment. This includes specifying external magnetic fields, electrical currents, and mechanical constraints. Proper application of boundary conditions ensures that the model behaves in a manner consistent with the physical system being studied. Various software tools, such as COMSOL Multiphysics, ANSYS Maxwell, and CST Studio Suite, are commonly used to perform these simulations, providing powerful capabilities for analyzing and optimizing electromagnetic systems.

Case studies and applications of FEM in electromagnetic systems demonstrate its capabilities and benefits. For instance, solenoid performance analysis can be conducted using FEM to understand how design changes affect the magnetic field distribution and resultant forces. This helps in optimizing the solenoid design for better performance and efficiency. In the design optimization of electromagnetic valves, FEM can be used to simulate different configurations and materials, identifying the most effective design for a given application. For example, Zhang [21] presented a study where a dual-coil solenoid valve for injection molding machines was designed and simulated using COMSOL software, demonstrating significant improvements in dynamic performance and a reduction in coil heat generation compared to conventional single-coil solenoid valves. Another important application is in studying magnetic field distribution within an actuator. FEM allows for detailed visualization of the magnetic field, providing insights into how it interacts with the actuator components and the surrounding environment. This information is critical for minimizing losses and maximizing the efficiency of the system.

In this thesis, COMSOL Multiphysics will be utilized extensively, leveraging specific modules tailored for electromagnetic simulations. The following modules will be employed:

- **Magnetic Fields**: This module is designed for analyzing magnetic fields and their interaction with materials and currents. It solves Maxwell's equations in their integral form, including the equations governing magnetic vector potential $\mathbf{A}$ and magnetic flux density $\mathbf{B}$:

$$\nabla \cdot \mathbf{B} = 0 \qquad \text{(Gauss's law for magnetism)} \tag{2.11}$$

$$\nabla \times \mathbf{B} = \mu_0 \mathbf{J} + \mu_0 \epsilon_0 \frac{\partial \mathbf{E}}{\partial t} \qquad \text{(Ampère's law with Maxwell's correction)} \tag{2.12}$$

  where $\mathbf{J}$ is the current density, μ_0 is the permeability of free space, and ϵ_0 is the permittivity of free space.

  Additionally, it computes the magnetic vector potential $\mathbf{A}$ and solves for the magnetic forces acting on conductors carrying currents, which are crucial for understanding electromagnetic actuators and devices.

- **Global ODEs and DAEs**: Useful for incorporating ordinary differential equations (ODEs) and differential algebraic equations (DAEs) into simulations, essential for dynamic electromagnetic systems.

- **Moving Mesh**: Enables the simulation of moving components, crucial for applications where the geometry changes during operation, such as actuators.

- **Heat Transfer in Solids**: This module provides tools to analyze heat transfer phenomena within solid materials, important for understanding thermal effects in electromagnetic devices.

These modules will facilitate comprehensive simulations to analyze and optimize electromagnetic systems, ensuring accurate representation of physical phenomena and supporting the design process effectively [22, 23].

2.4 Sensitivity and Parameter Analysis in Electromechanical Systems

Sensitivity analysis is a crucial aspect of modeling and simulation in electromechanical systems. It provides insights into how variations in parameters affect system behavior, enabling engineers to identify which parameters have the most significant impact on performance. This knowledge is vital for optimizing system design, improving reliability, and find parameters that allow robust operation under varying conditions. Analytical techniques for sensitivity analysis involve mathematical and computational methods to quantify how changes in input parameters influence output responses. Sensitivity coefficients, response surface methodologies, and uncertainty quantification techniques such as Monte Carlo simulations and bootstrap methods are commonly used. These methods help build a thorough understanding of the system's behavior, guide the optimization process, and ensure the model's reliability under uncertain conditions.

In this thesis, sensitivity analysis is applied to evaluate three critical curves indicative of faults in solenoid valves, obtained from simulation results. The first curve analyzes the dependence of the initial slope $mvAn$ on the stroke (end position). The second curve examines the dependence of the flux linkage Ψ_{diff} at a current of $I = 1$ A on the residual air gap (engaged state). The third curve focuses on the dependence of the starting flux Ψ_{start} at the beginning of the movement on the friction force. By analyzing how variations in parameters such as initial position, stroke, friction, return spring, and temperature impact these curves, the study aims to optimize the design for improved reliability, efficiency, and fault tolerance. Additionally, the curves obtained from the simulations will be compared with those obtained experimentally in the project SmartValve [3], ensuring the validity and accuracy of the simulation results.

2.5 Previous Works and the SmartValve Project

The SmartValve project represents a significant innovation in the research and development of electromagnetic fluid valves, emphasizing condition monitoring and performance optimization. This initiative focuses on creating advanced models to predict valve behavior, implementing real-time monitoring techniques, and improving system reliability and efficiency. Key

outcomes include enhanced predictive accuracy and diagnostic capabilities, though challenges persist in integrating diverse monitoring techniques and developing robust models for varying operational conditions. Future research directions propose refining modeling techniques, integrating machine learning for predictive maintenance, and exploring novel materials and designs [3].

While the SmartValve project introduces groundbreaking methodologies, it is essential to place this research in the context of other studies in the field. Comparative analyses reveal that Finite Element Analysis (FEA) and advanced sensor technologies are widely adopted for accurate modeling and real-time monitoring of electromagnetic fluid valves. These studies underscore the importance of multidisciplinary approaches and holistic frameworks combining electrical, mechanical, and thermal analyses. However, most of the existing work lacks the integration of 3D transient simulations with parameter studies and sensitivity analyses, which are key contributions of the present research. Furthermore, the standardization of testing protocols remains a significant gap, often leading to discrepancies between simulation results and experimental data.

This research builds upon the foundational work of SmartValve and addresses limitations in existing literature by introducing a comprehensive modeling approach that integrates 3D FEM simulations, parameter studies, and experimental validation, bridging the gap between theoretical modeling and practical application.

3 Computational Modelling and Analysis Methodology

3.1 Case Study Description: Industrial Fluid Valve from the SmartValve Project

The SmartValve project aims to enhance the performance and reliability of industrial fluid valves through advanced modelling and simulation techniques. This case study focuses on a specific type of industrial fluid valve used in high-demand applications, such as automotive, aerospace, and manufacturing industries. These valves are critical components in fluid control systems, where precision and reliability are paramount.

The chosen valve for this study is the RSG 270 series coaxial 2/2 way direct acting solenoid valve, for which we obtained the 3D geometry in a CAD file from the SmartValve project. The valve operates using an electromagnetic actuator, which converts electrical energy into mechanical motion to regulate the flow of fluids. The primary goal of this study is to develop a comprehensive multi-domain model of the valve, integrating electromagnetic, mechanical, and thermal aspects to accurately predict its behaviour under various operational conditions. This integrated approach is essential for understanding the complex interactions within the valve and for optimizing its design and performance.

We previously showed the valve and its components in Figure 2.9, and we will revisit this edited as Figure 3.1 in this section to indicate the relevant magnetic components.

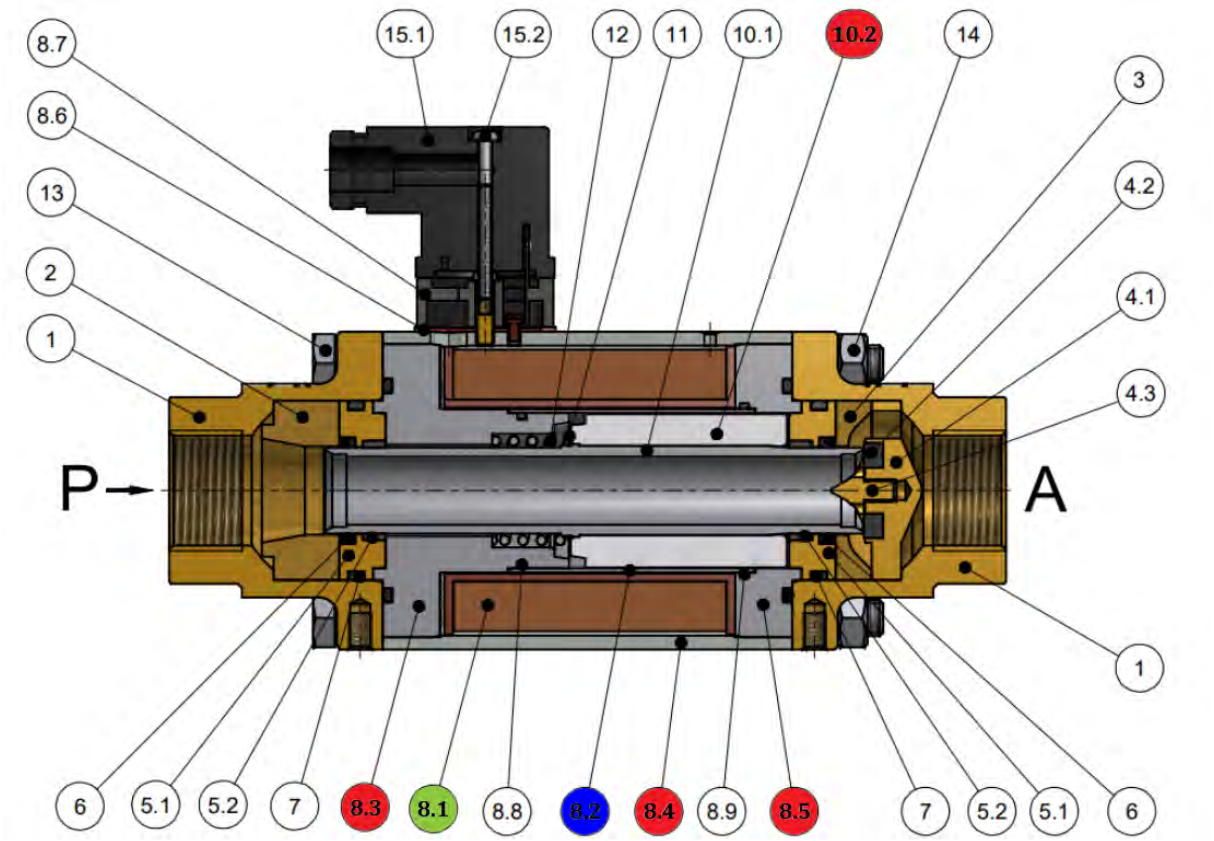

Figure 3.1: Cross-sectional view of a directly controlled coaxial valve from the 270 DN15 series, adapted from [13]. The figure highlights the relevant components: (red) ferromagnetic, (blue) weakly magnetizable, and (green) non-magnetizable, used in the simulation.

To achieve the objectives of this study, we will employ Finite Element Method (FEM) simulations to model the magnetic circuit of the valve and to calculate the resulting forces on the piston rod. Additionally, we will perform parameter studies to evaluate the impact of various mechanical parameters, such as initial position, stroke, friction, return spring, and temperature, on the valve's performance. The insights gained from these studies will contribute to the development of more efficient and reliable fluid control systems.

The case study's significance lies in its potential to reduce engineering time and costs by minimizing the need for extensive experimental testing. By leveraging advanced simulation tools, we aim to provide a deeper understanding of the valve's behaviour and to identify opportunities for performance improvements and cost savings.

Table 3.1 lists the physical properties of the valve relevant to the study.

Table 3.1: Physical properties of the RSG 270 series coaxial valve relevant to the system simulation.

Physical Property	**Symbol**	**Value**	**Details**
Anchor Mass	m_A	320g	Anchor + guide rod
Moving Mass	m_{Mess}	486g	Moving mass in the test setup
Residual Air Gap	δ_0	0.3mm	Thickness of the anti-adhesive disc
Anchor Stroke	Δx	3.1mm	Nominal
Spring Stiffness	c_F	5.4N/mm	
Spring Preload	F_{F0}	54.54N	Unstressed length $L_0 = 27$ mm, installation length $L = 16.9$ mm
Operating Voltage	U_B	24V	Nominal voltage
Number of Turns	N	1430	
Wire Diameter	d_{Dr}	0.6mm	
Coil Resistance	R	13.5Ω	Ohmic resistance at 20°C
Nominal Current	I	1.78A	Stationary current at U_B and R
Magnetomotive Force	Θ	2542A	$N \cdot I$
Inductance	L	55mH	

Table 3.2 lists the components of the valve used in the simulation, including their materials and descriptions.

Table 3.2: Components of the RSG 270 series coaxial valve used in the simulation.

Item	**Component**	**Material**	**Description**
8.3	Magnet Core	9SMn28k	B-H curve in Figure 3.2
8.5	Magnet Cap	9SMn28k	B-H curve in Figure 3.2
10.2	Push Sleeve	9SMn28k	B-H curve in Figure 3.2
8.4	Coil Housing	St35-2	Unalloyed structural steel
8.1	Coil/Coil Body	Wound	

Since the material 9SMn28k is not available in the Comsol software component library, we created this material based on the B-H curve data provided by the SmartValve project. The B-H

curve for the 9SMn28k material, as created in Comsol, is shown in Figure 3.2.

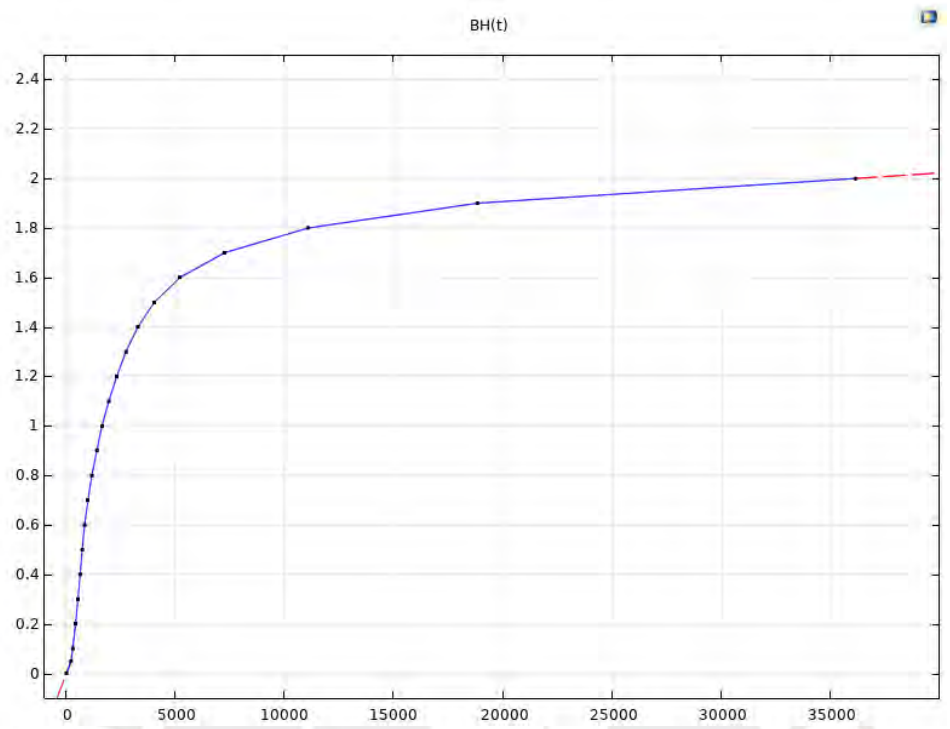

Figure 3.2: B-H curve of the 9SMn28k material created in Comsol

3.2 3D Modelling of the Valve's Magnetic Circuit

The 3D modelling of the valve's magnetic circuit is essential for predicting its operational efficiency and reliability. This section outlines the steps involved in developing and simulating the 3D model using COMSOL Multiphysics.

The CAD model of the valve mentioned in section 3.1 served as the basis for this modelling effort. Components detailed in Table 3.2 were imported into COMSOL Multiphysics for the simulation process.

3.2.1 Initial Simulation Setup

The CAD geometry of the valve components, as listed in Table 3.2, was created in SolidWorks and imported into COMSOL Multiphysics for simulation. The process of creating each component's geometry is detailed below:

Coil Housing The coil housing geometry was created starting with the sketch shown in Figure 3.3. Symmetry was applied to the visible entities with respect to Line 2. A solid revolution was then created using Line 1 as the axis of revolution.

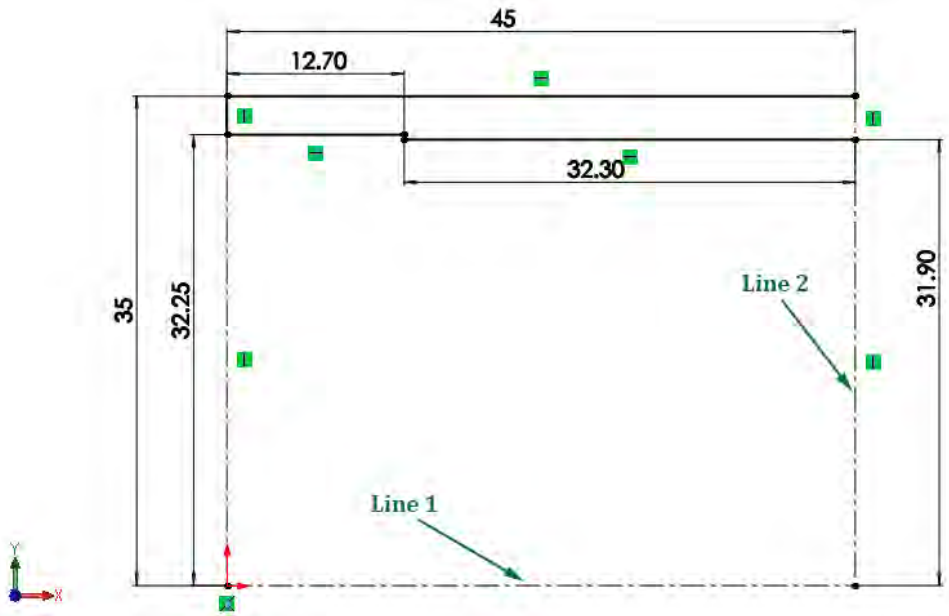

Figure 3.3: Coil housing sketch in SolidWorks.

Coil The coil geometry was created based on the sketch shown in Figure 3.4. A solid revolution was performed using Line 1 as the axis of revolution.

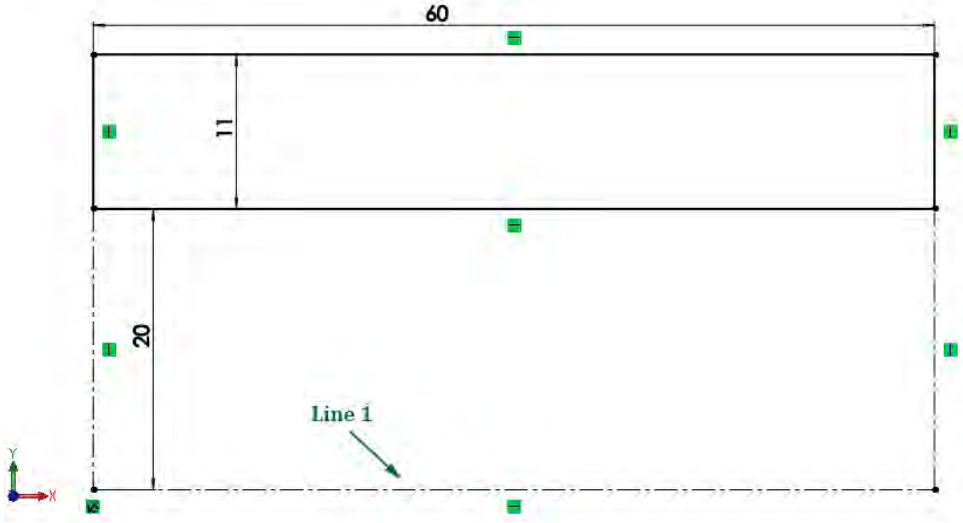

Figure 3.4: Coil sketch in SolidWorks.

Magnet Cap The magnet cap was designed using the sketch shown in Figure 3.5. A solid revolution was performed using Line 1 as the axis of revolution.

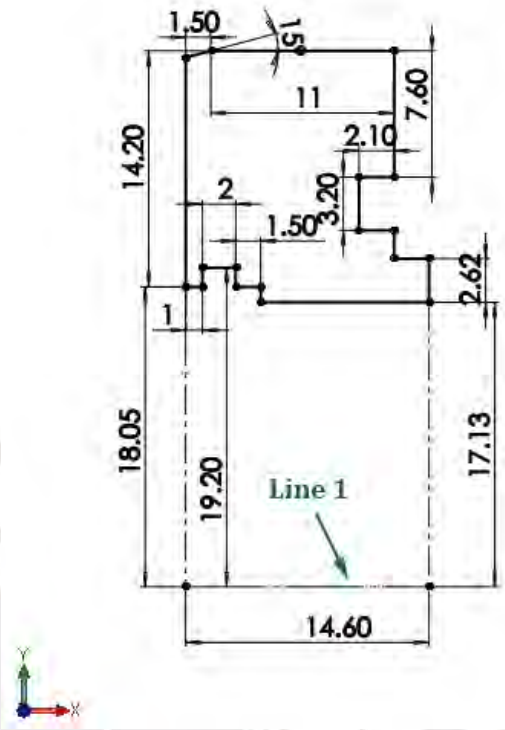

Figure 3.5: Magnet cap sketch in SolidWorks.

Magnet Core The magnet core geometry was created using the sketch in Figure 3.6. A solid revolution was created using Line 1 as the axis of revolution.

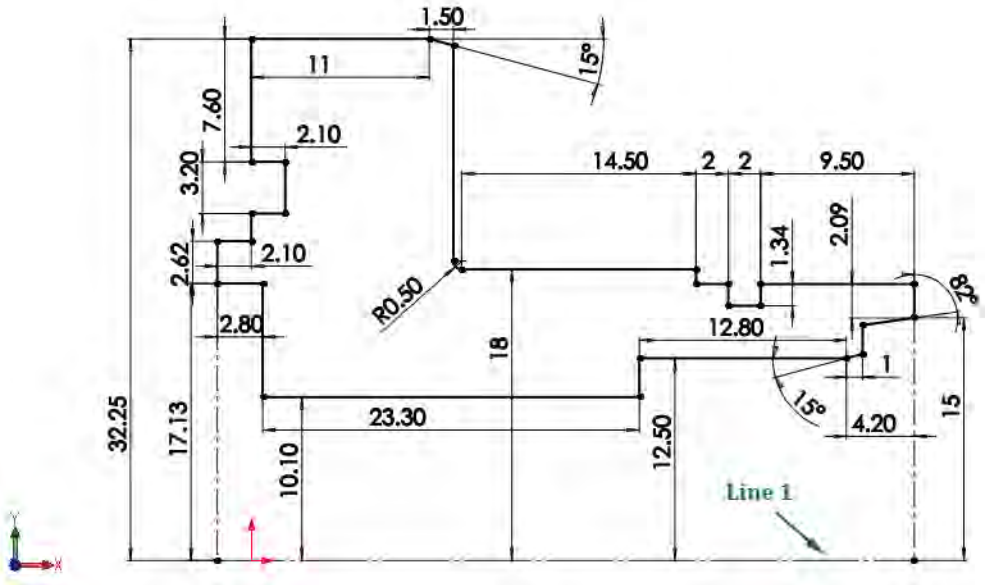

Figure 3.6: Magnet core sketch in SolidWorks.

Push Sleeve The push sleeve was modelled from the sketch shown in Figure 3.7. A solid revolution was performed using Line 1 as the axis of revolution.

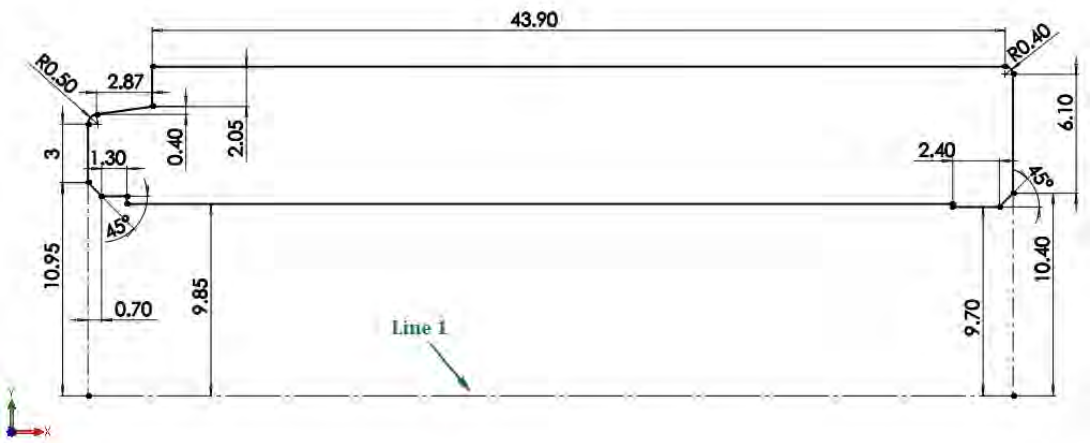

Figure 3.7: Push sleeve sketch in SolidWorks.

Assembly of the Magnet Finally, all the individual components were imported into COMSOL Multiphysics and assembled as shown in Figure 3.8. The positions of each component were carefully aligned to replicate the real geometry of the valve.

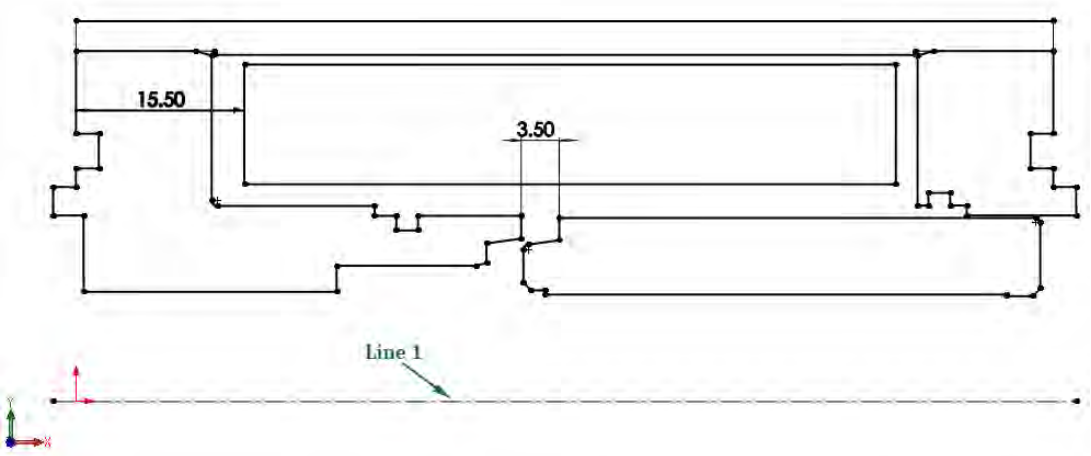

Figure 3.8: Assembly of the valve components in COMSOL Multiphysics.

The imported geometry was then meshed to create a finite element mesh, essential for discretizing the domain into smaller elements. This setup included the Magnetic Fields module. Figure 3.9 presents the results from the initial simulation with a 24V voltage source applied, illustrating the distribution of Magnetic Flux Density Norm (MFDN) in both 3D and 2D formats within the valve's geometry.

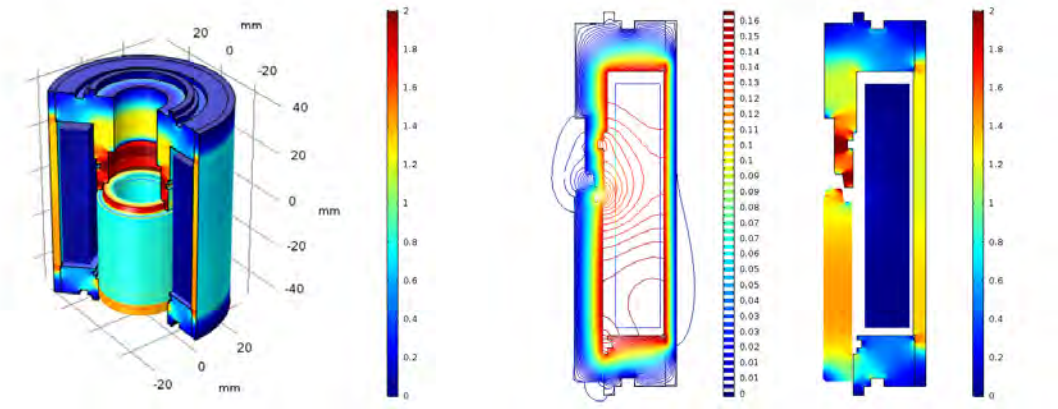

(a) 3D Magnetic Flux Density Norm (T). (b) 2D Magnetic Flux (Wb) and MFDN (T).

Figure 3.9: MFDN with real geometry.

3.2.2 Geometry Optimization

The optimization process was carried out with a qualitative approach, focusing on simplifying the geometry to eliminate narrow air gaps and complex features that could introduce meshing difficulties and numerical singularities. This approach ensures a balance between computational efficiency and model fidelity without compromising the accuracy of the results.

Coil Housing

The sketch shown in Figure 3.10 was created. Symmetry of the visible entities was applied with respect to Line 2. A revolution solid was generated using Line 1 as the axis.

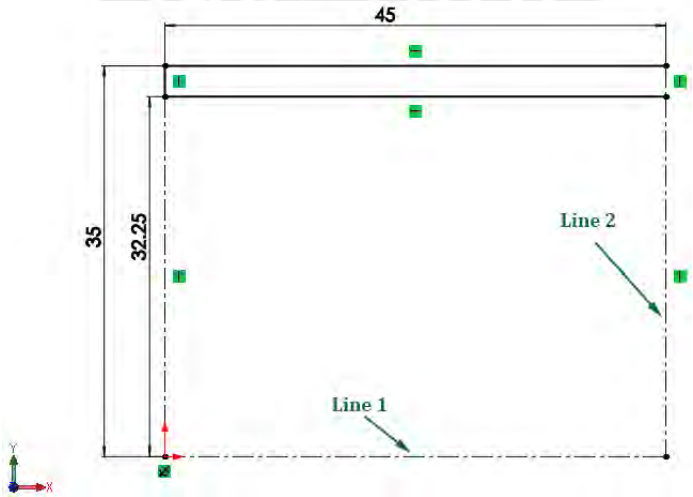

Figure 3.10: Coil housing sketch in SolidWorks.

Magnet Cap

The sketch shown in Figure 3.11 was created. A revolution solid was generated using Line 1 as the axis.

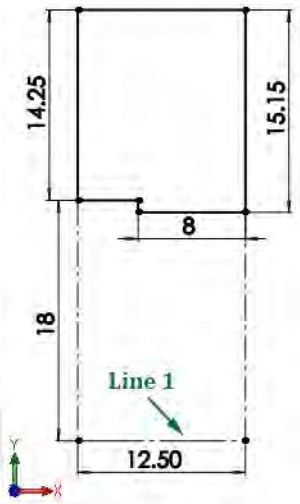

Figure 3.11: Magnet cap sketch in SolidWorks.

Magnet Core

The sketch shown in Figure 3.12 was created. A revolution solid was generated using Line 1 as the axis.

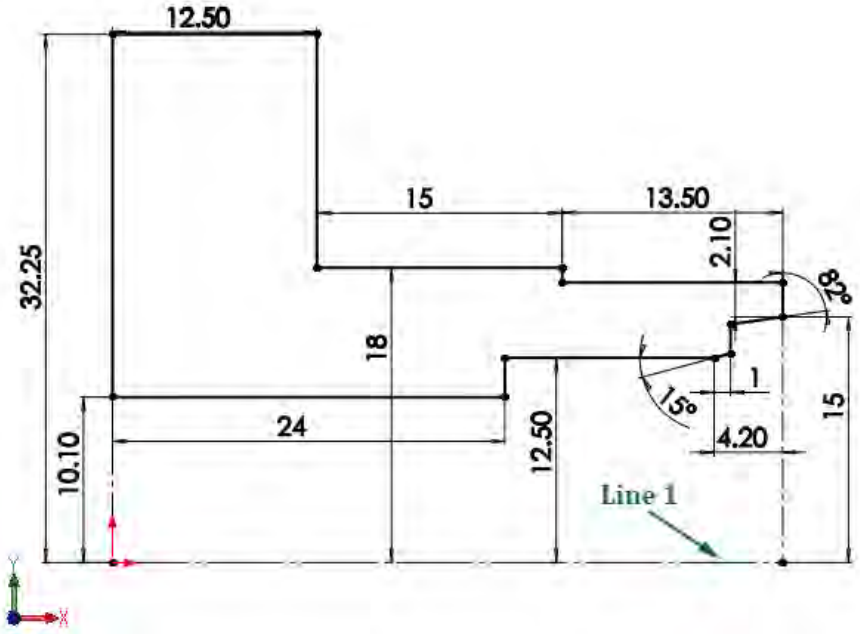

Figure 3.12: Magnet core sketch in SolidWorks.

Push Sleeve

The sketch shown in Figure 3.13 was created. A revolution solid was generated using Line 1 as the axis.

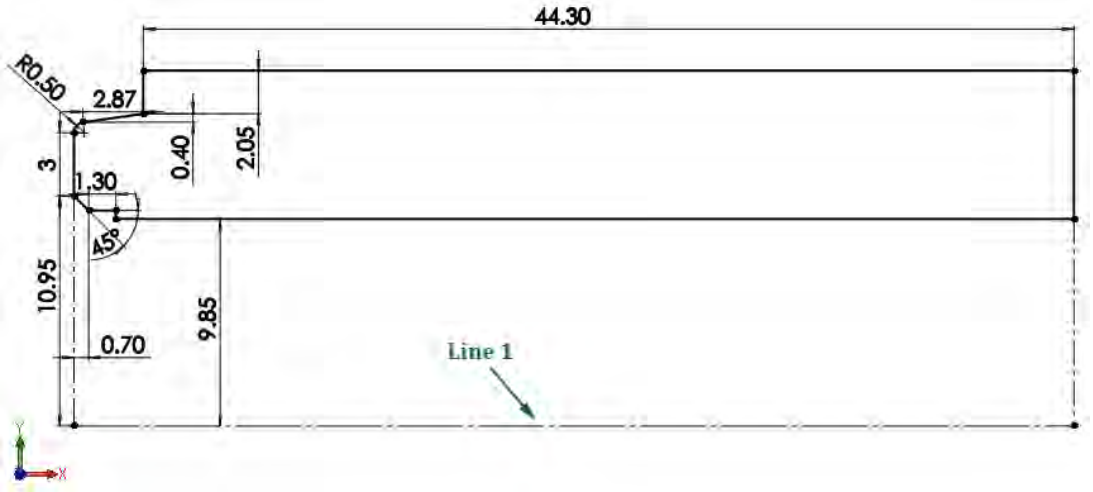

Figure 3.13: Push sleeve sketch in SolidWorks.

Assembly of the Magnet

Finally, these modified components were imported into COMSOL and assembled in the positions shown in Figure 3.14.

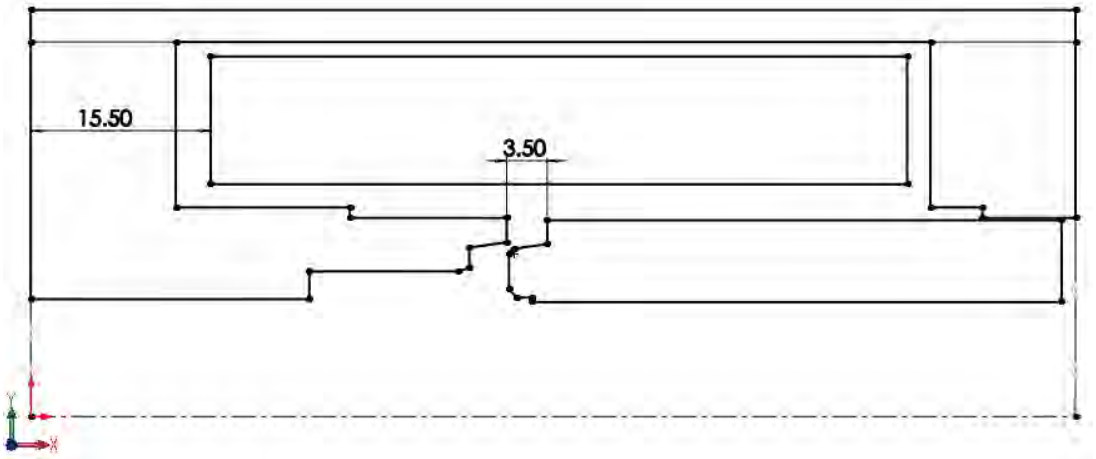

Figure 3.14: Final assembly of the magnet in COMSOL.

The modifications performed include:

- Elimination of air gaps between components.

- Simplification of certain parts of the model to facilitate meshing.

To illustrate the impact of these modifications, Figure 3.15 presents a comparison of simulation time between the original and optimized geometries.

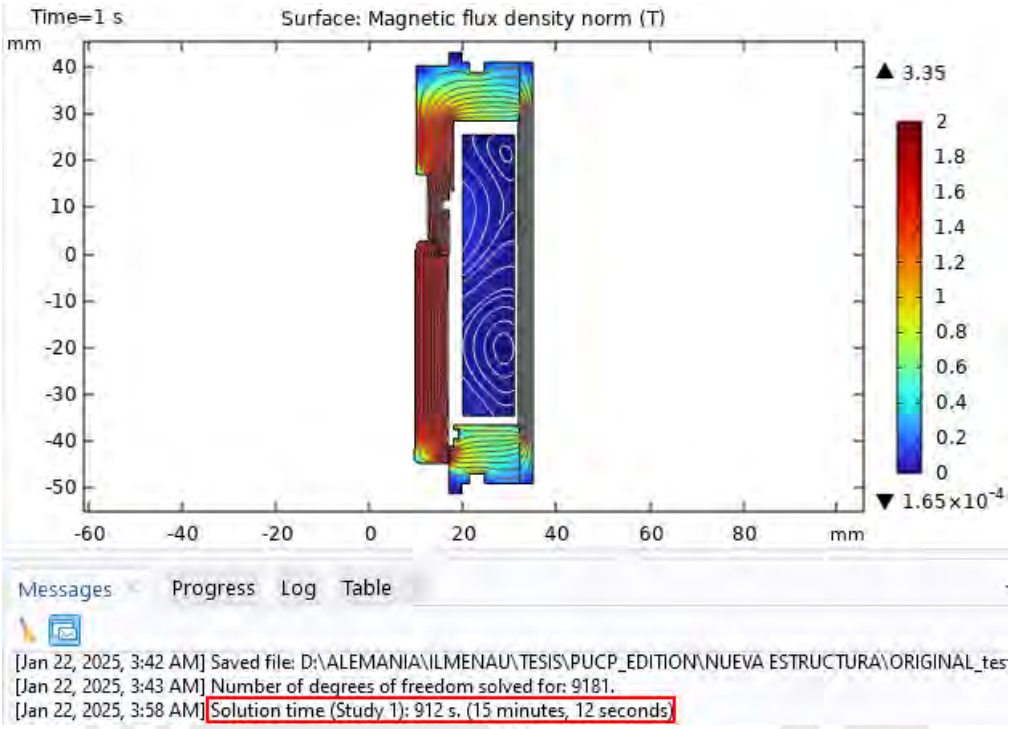

(a) Original geometry simulation time.

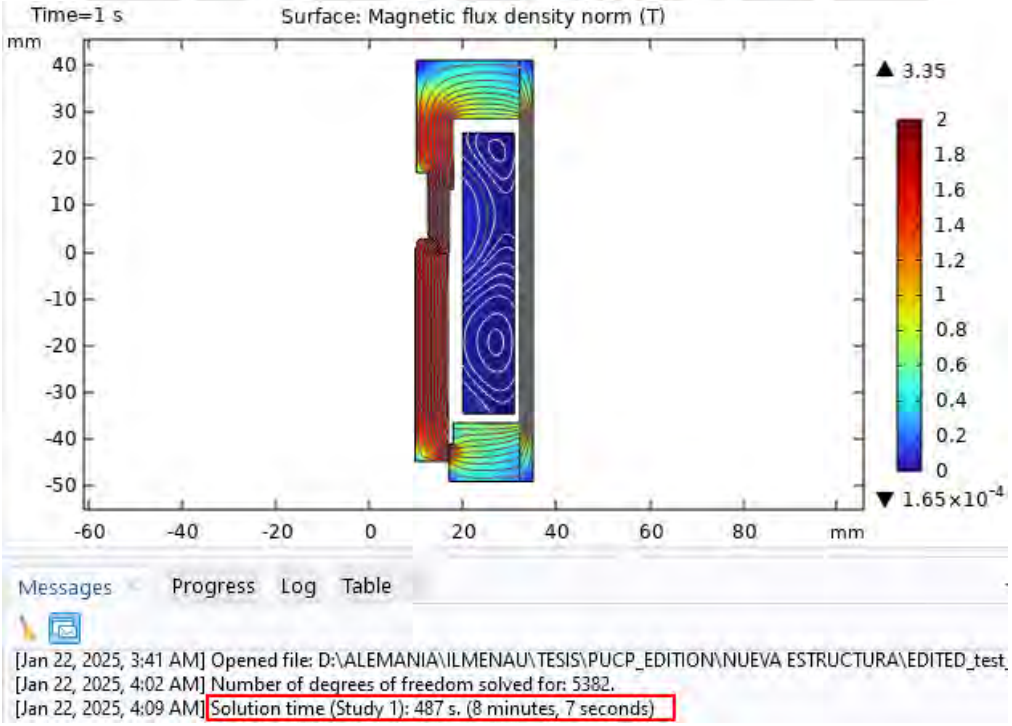

(b) Optimized geometry simulation time.

Figure 3.15: Comparison of simulation time.

A reduction in processing time of 425 seconds was observed, resulting in a 47% reduction in simulation time. Although this time may not seem significant, the cumulative effect over hundreds of simulations with varying parameters makes this time reduction crucial. Additionally, these modifications helped prevent numerical errors and simulation failures, further improving the robustness of the computational analysis.

Defining domains in COMSOL is a crucial step, as it enables the assignment of material properties to each component, thereby determining their magnetic characteristics. This process was carried out before initiating the simulations. Figure 3.16 presents the resulting domains after implementing the optimized geometry.

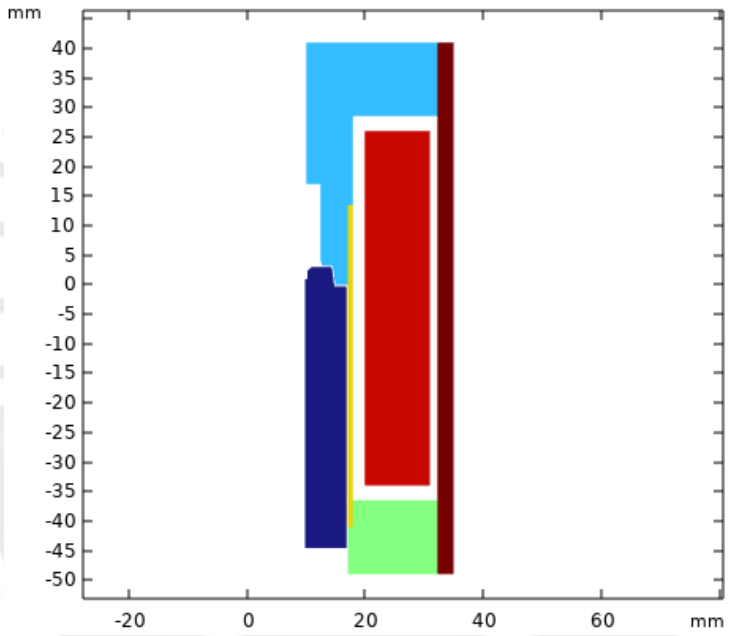

Figure 3.16: Domain setup in COMSOL Multiphysics after geometry modification.

3.2.3 Meshing

Careful attention was given to the meshing process to balance computational effort and result resolution. Parameters were adjusted to ensure computational efficiency without sacrificing result accuracy. Figure 3.17 illustrates the meshing setup in COMSOL Multiphysics, highlighting the balance achieved between computational effort and result resolution. This process is meticulous, as improper setup may lead to computational singularities and hours of simulation ending in errors.

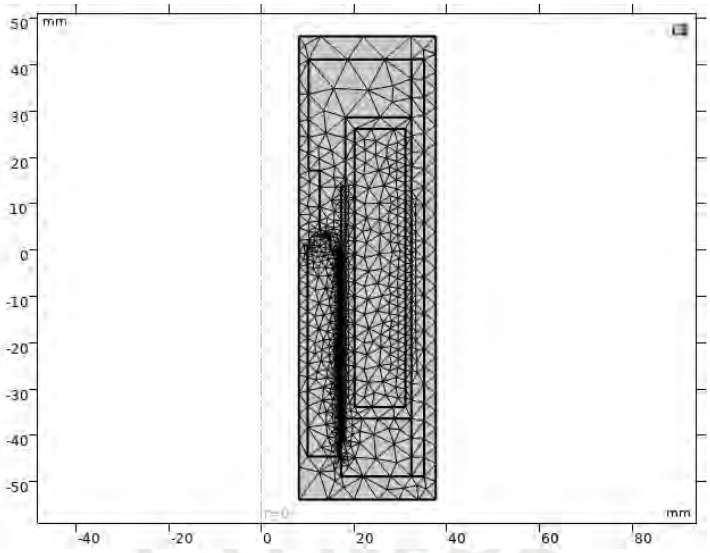

Figure 3.17: Meshing setup in COMSOL Multiphysics.

To ensure that the obtained results are independent of the mesh element size, a **mesh convergence study** was performed. The simulation was conducted using progressively coarser meshes, starting from an extremely fine mesh and increasing the element size step by step. The force acting on the moving component was recorded for each case.

Figure 3.18 presents the variation of the computed force over time for different mesh densities. Additionally, Table 3.3 summarizes the effective force obtained for each mesh size and the relative error between consecutive refinements.

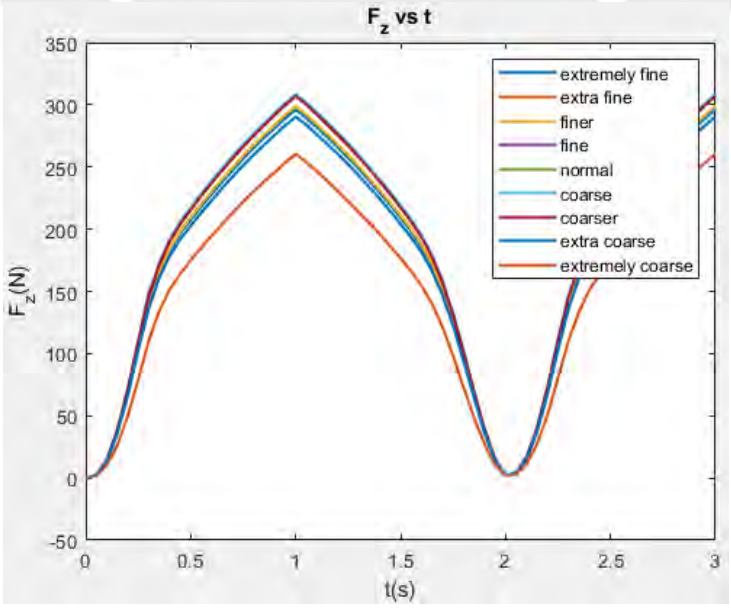

Figure 3.18: Mesh convergence study: force variation with different mesh densities.

Table 3.3: Mesh convergence study: effective force and relative error.

Mesh Size	**Effective Force (N)**	**Relative Error (%)**
Extremely Fine	203.03	-
Extra Fine	204.83	0.89
Finer	204.88	0.02
Fine	211.40	3.18
Normal	211.11	0.14
Coarse	212.32	0.57
Coarser	210.68	0.77
Extra Coarse	198.57	5.75
Extremely Coarse	173.87	12.44

The results indicate that for meshes finer than **Coarser**, the relative error remains below 1%, confirming that the simulation results are mesh-independent. Based on this analysis, the **Normal** mesh size was selected for the simulations, as it maintains a relative error below 1% while avoiding the increased computational cost associated with finer meshes such as **Finer**.

Similarly, a **time-step sensitivity analysis** was conducted to verify the independence of the results from the time discretization. Several simulations were performed using different time-step sizes, and the results were compared. Figure 3.19 illustrates the variation in computed force with different time-step values.

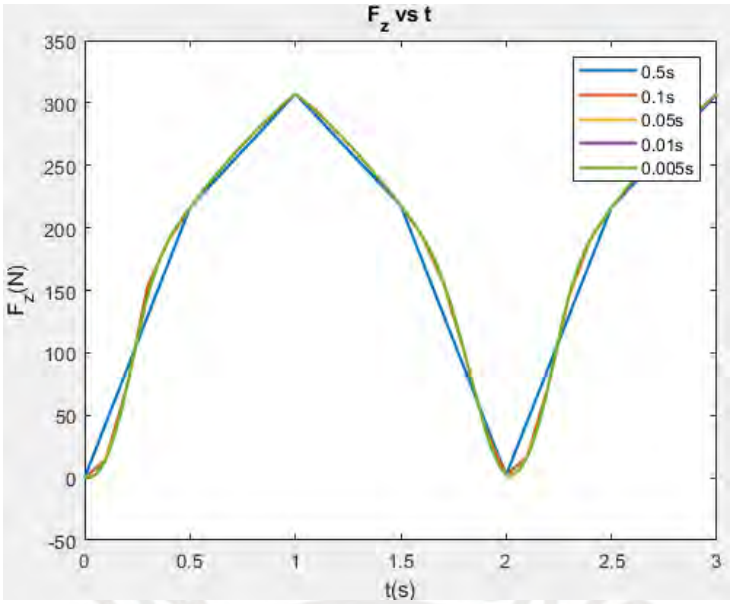

Figure 3.19: Time-step sensitivity analysis: force variation with different time-step values.

To complement the graphical analysis, Table 3.4 summarizes the effective force values obtained for each time-step size, along with the relative error between consecutive refinements.

Table 3.4: Time-step sensitivity study: effective force and relative error.

Time Step (s)	**Effective Force (N)**	**Relative Error (%)**
0.5	216.99	-
0.1	211.53	2.52
0.05	211.11	0.20
0.01	211.02	0.04
0.005	211.01	0.01

The results indicate that for time steps smaller than **0.1s**, the relative error remains below 1%, ensuring time-step independence. Based on this analysis, a time-step of **0.05s** was selected as the optimal balance between accuracy and computational efficiency.

Both studies confirm that the selected meshing and time-step configurations yield results that are **mesh and time-step independent**, ensuring the reliability of the simulation outcomes.

Each stage of the simulation process aimed to deepen understanding of the valve's magnetic circuit behavior under varying operational conditions, contributing to its design and performance optimization.

3.3 Calculation of Transverse Forces at Non-Coaxial Positions

In the operation of an electromagnetic fluid valve, understanding the forces acting on the components is essential, particularly when these components are not in their ideal coaxial positions. Transverse forces arise primarily due to misalignment or lateral displacement of the piston rod. These misalignments can result from various causes, including manufacturing tolerances, assembly errors, or wear and deformation over time.

In this study, we focus on the case where the plunger is inclined due to the deformation or wear of the valve seals 5.2 and 6 made of PTFE (see Table 2.1). Although such failures are rare, they can lead to significant performance degradation. It was calculated that the inclination due to this failure is 0.11°CCW along the z-axis. Based on this, the geometry was modified in SolidWorks to incorporate this inclination. Figure 3.20 shows the points of contact in these failures.

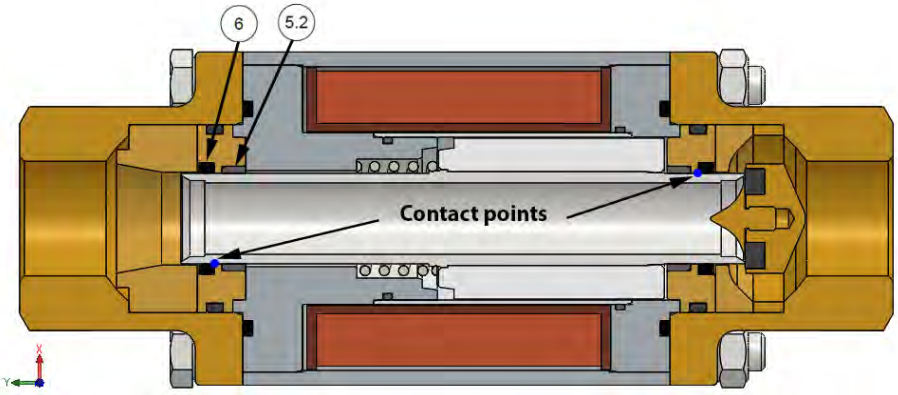

Figure 3.20: Points of contact in the valve failures due to seal deformation.

The complete 3D geometry with the inclined plunger was imported into COMSOL Multiphysics. However, the computational process required days of simulation, often encountering singularities that halted the process. Initially, the complete 3D geometry was used because the plunger's inclination disrupted the axial symmetry of the system. Upon further analysis, it was observed that the system retained symmetry with respect to the xy-plane, as detailed in the previous figure.

Consequently, the geometry was modified again in SolidWorks, and one half was exported to

COMSOL for simulation. Figure 3.21 shows the imported geometry and meshing setup in COMSOL.

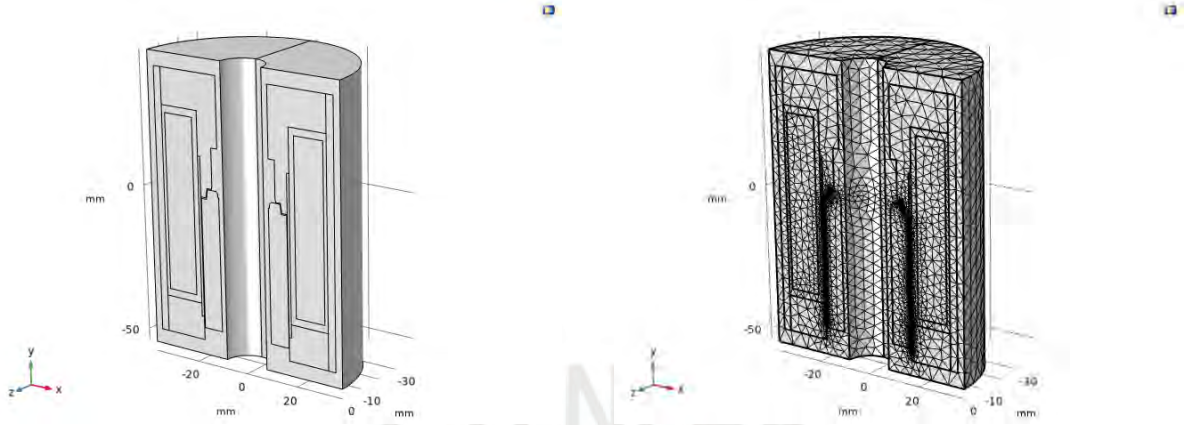

(a) Imported geometry with inclined plunger. (b) Meshing setup in COMSOL Multiphysics.

Figure 3.21: Imported geometry and meshing setup in COMSOL for non-coaxial plunger.

The software solves the modified Maxwell's equations to reflect the new boundary conditions. The resulting magnetic flux distribution is then used to compute the magnetic force components acting in the transverse direction.

The transverse forces are evaluated by integrating the magnetic stress tensor over the surface of the plunger in its inclined position. This integration provides a quantitative measure of the forces that act perpendicular to the rod's axis. These forces are analysed to determine their dependence on the extent of misalignment and the operating conditions of the valve.

The results of these calculations will be critical for identifying potential issues related to misalignment. High transverse forces can lead to increased friction, wear, and potential mechanical failure. By understanding these forces, design modifications can be proposed to mitigate their effects, such as improving the guidance system for the plunger or enhancing the structural integrity of the valve components.

3.4 2D Modelling of the Magnetic Circuit

2D modelling of the magnetic circuit offers a simplified yet insightful approach to understanding the electromagnetic behaviour of the valve. This method is particularly useful for analysing the effects of electrical excitation and mechanical parameters on the transient behaviour of the

system. Given that the system is axially symmetric, COMSOL Multiphysics allows for 2D modelling, which reduces computational complexity and simulation time.

3.4.1 Integration of Electrical Excitation

The 2D model is created by extracting a cross-sectional view of the valve's magnetic circuit, preserving the essential characteristics of the magnetic field distribution while simplifying the computational effort. In COMSOL, the plunger is positioned in its minimum position with an air gap of 0.3mm, representing the fully open valve with the spring compressed and the plunger touching the anti-remanence disc 11 (see Table 2.1).

The current source is made variable, and the coil is excited for a duration of 3 seconds. This setup allows for the observation of the magnetic flux density throughout the geometry. The flux linkage, Ψ, is calculated using the following equation:

$$\Psi = N \cdot S_p \cdot B_z \tag{3.1}$$

where Ψ is the flux linkage in Wb, S_p is the cross-sectional area of the plunger in m^2, B_z is the magnetic field intensity in T, and N is the number of turns in the coil.

Figure 3.22 shows the magnetic flux density and the flux linkage over time. The purpose of this excitation is to account for eddy currents; therefore, only the results obtained after the first second are considered.

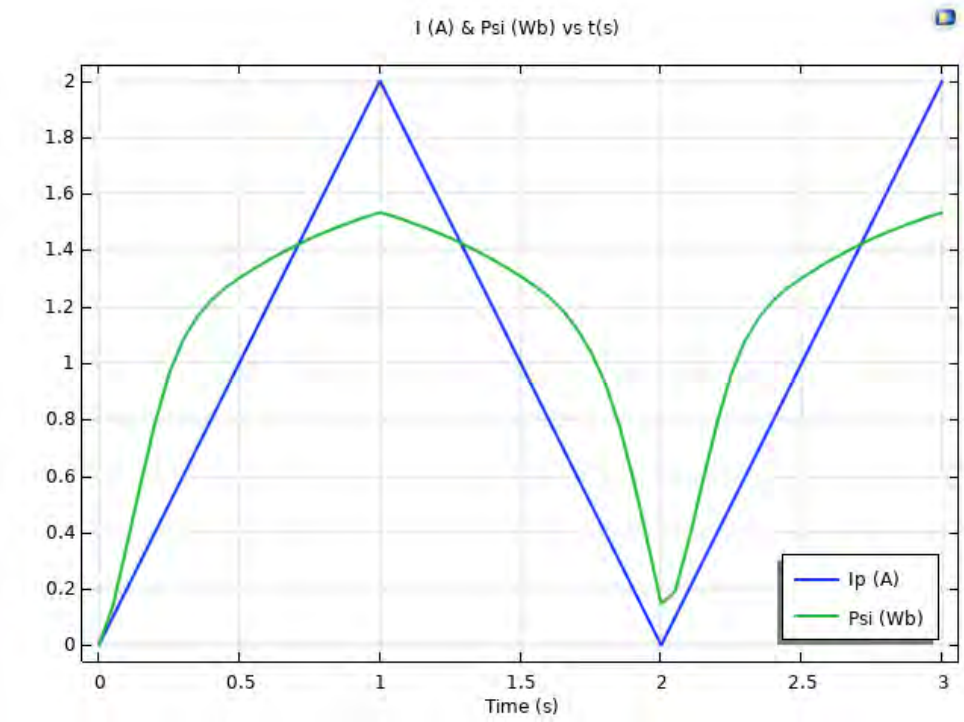

Figure 3.22: Current I_p and flux linkage Ψ vs. time.

3.4.2 Mechanical Parameters for Transient Simulations

The transient behaviour of the valve is influenced by various parameters, including the initial position of the piston rod, the stroke length, friction, return spring stiffness, and temperature. These factors are incorporated into the 2D model to study their impact on the valve's performance.

The geometry was prepared to vary the plunger position during simulations using the Moving Mesh module in COMSOL. Additionally, the Global ODEs and DAEs module was configured to handle variations in position and current over time.

Initial position and stroke length are varied to observe their effects on magnetic force generation and the variation of the characteristic curves Ψ vs. I. Friction is modelled as a damping force opposing the motion of the piston rod, and its impact on the magnetic behaviour of the valve is analysed. The return spring stiffness is included to evaluate its influence on the magnetic characteristics when the valve returns to its original position after actuation.

Temperature variations are also considered, as they affect material properties and the electrical

resistance of the solenoid coil. For these simulations, the Heat Transfer in Solids module of COMSOL is used. This approach helps to understand how temperature changes impact the magnetic behaviour and performance of the valve.

3.4.3 Data Acquisition for Dynamics Simulation

To accurately capture the dynamic behavior of the valve in simulations conducted using COMSOL Multiphysics, comprehensive data acquisition is crucial. This process involves systematically varying the plunger position x and excitation current I_p of the coil to explore their effects on magnetic flux linkage Ψ and electromagnetic force F_z, considering the theory seen in section 2.1.2.

The procedure for data acquisition is as follows (see Figure 3.23):

1. Set the plunger to the initial position $x = -0.1$ mm.
2. Apply the current to the coil as shown in Figure 3.22.
3. Save the resulting data to a .txt file.
4. Increase the plunger position to the next value.
5. Repeat steps 2, 3 and 4 until the plunger reaches the final position.

The current I varies in steps from 0.1 A to 2 A, and the plunger position x ranges from -0.1 mm to 3.2 mm. The purpose of taking values beyond the normal operating range of the valve ($x \in [0, 3.1]$ mm) is to obtain a wider range of values for F and Ψ.

All data were exported sequentially to a data.txt file. This file will be used for post-processing in Matlab and to study the behaviour of the Ψ vs I curve for cases where the initial position, stroke, friction, and return spring are variable. For cases with temperature variation, the data acquisition process varies slightly and will be explained in the next section.

Case with Variable Temperature

The process for data acquisition with variable temperature is as follows (see Figure 3.24):

1. Set the temperature of the coil.

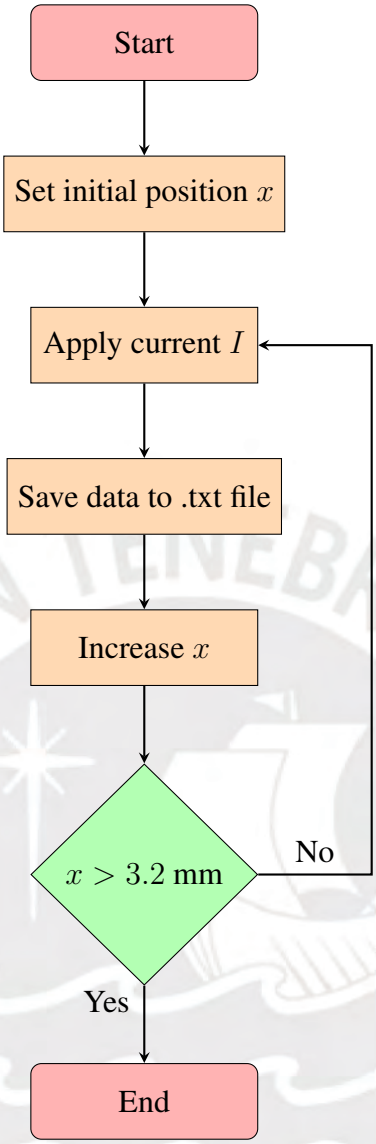

Figure 3.23: Flowchart of the process to obtain data from COMSOL simulations.

2. Set the plunger to the initial position $x = -0.1$ mm.
3. Apply the current to the coil as shown in Figure 3.22.
4. Save the resulting data to a data_T.txt file.
5. Increase the plunger position to the next value.
6. Repeat steps 3, 4, and 5 until the plunger reaches the final position.
7. Increase the temperature.
8. Return to step 2 until the maximum analysis temperature is reached ($T_{\text{max}} = 80°\text{C}$).

This time, the Heat Transfer in Solids module will be used to account for temperature variations.

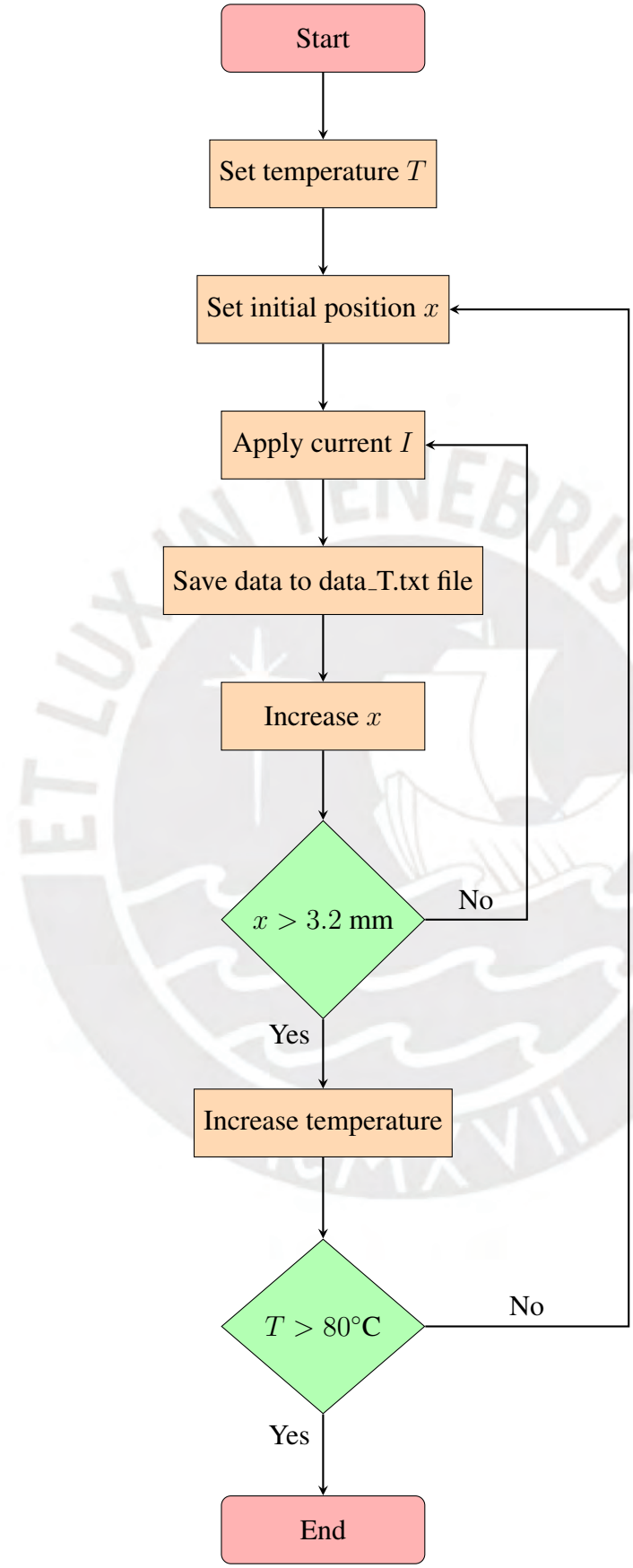

Figure 3.24: Flowchart of the process to obtain data from COMSOL simulations with variable temperature.

Feasibility Analysis of Direct Characteristic Curve Extraction in COMSOL

The ideal scenario would involve extracting all characteristic curves directly within COMSOL by varying all mechanical parameters within the software. To analyze the feasibility of this process, an algorithm is developed to find the Ψ vs I characteristic curve (refer to Figure 2.7).

Falling Off Process The falling off process is defined as follows:

- Set initial values: position $z = 0$ mm, velocity $v_z = 0$ mm/s, current $I = 0$ A, current rate $v_I = 1$ A/s.
- Start simulation.
- Stop condition: $F_z > F_r + F_{k0}$, where F_z: magnetic force, F_r: friction force, F_{k0}: spring preload.

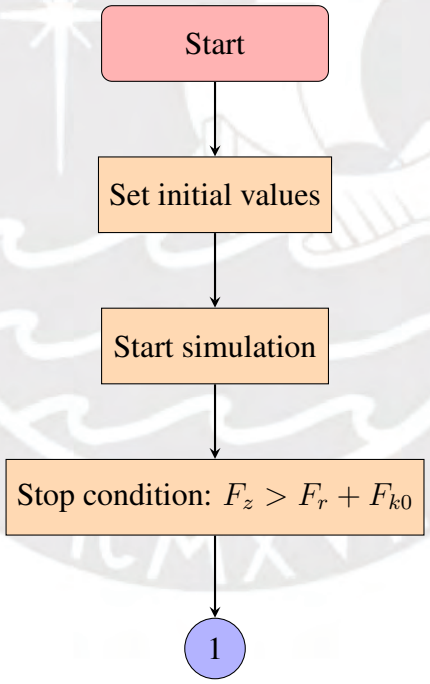

Figure 3.25: Flowchart of the Falling Off process for characteristic curve extraction in COMSOL.

Magnetization Process The magnetization process is more complex and is described as follows:

- Set: velocity $v_z = 3.1$ mm/s, current rate $v_I = 0$ A/s, during $\Delta t = 0.1$ s.

- Perform: velocity $v_z = 0$ mm/s, current rate $v_I = -0.1$ A/s.
- Repeat while $F_z > F_r + F_{k0}$.
- If $z < 3.1$ mm, return to step 1. Otherwise, stop the process.

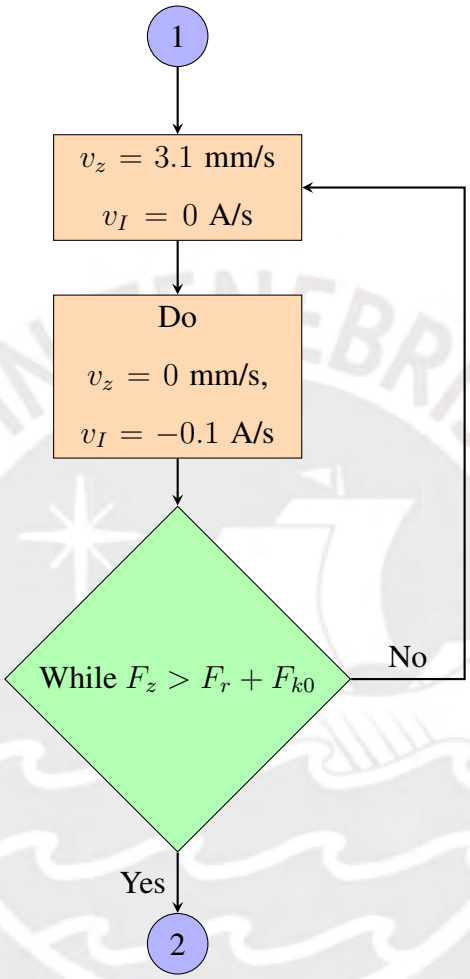

Figure 3.26: Flowchart of the Magnetization process for characteristic curve extraction in COMSOL.

Attraction Process The attraction process is defined as follows:

- Set velocity $v_z = 0$ mm/s, current rate $v_I = 0.25$ A/s.
- Stop condition: $I > 1.77$ A.

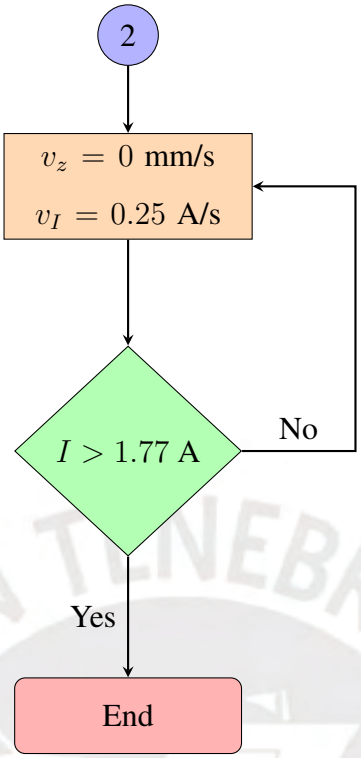

Figure 3.27: Flowchart of the Attraction process for characteristic curve extraction in COMSOL.

Although an attempt was made to automate the simulation, it was not possible to obtain the data in the *Magnetization process* sequentially, so this process had to be segmented and simulations had to be run for each variation of the plunger position until it reached its maximum position. Therefore, this process was divided into 10 steps.

It is explained that ODEs must be implemented for each subprocess. Figure 3.28 shows ODEs implemented for each subprocess in the magnetization process:

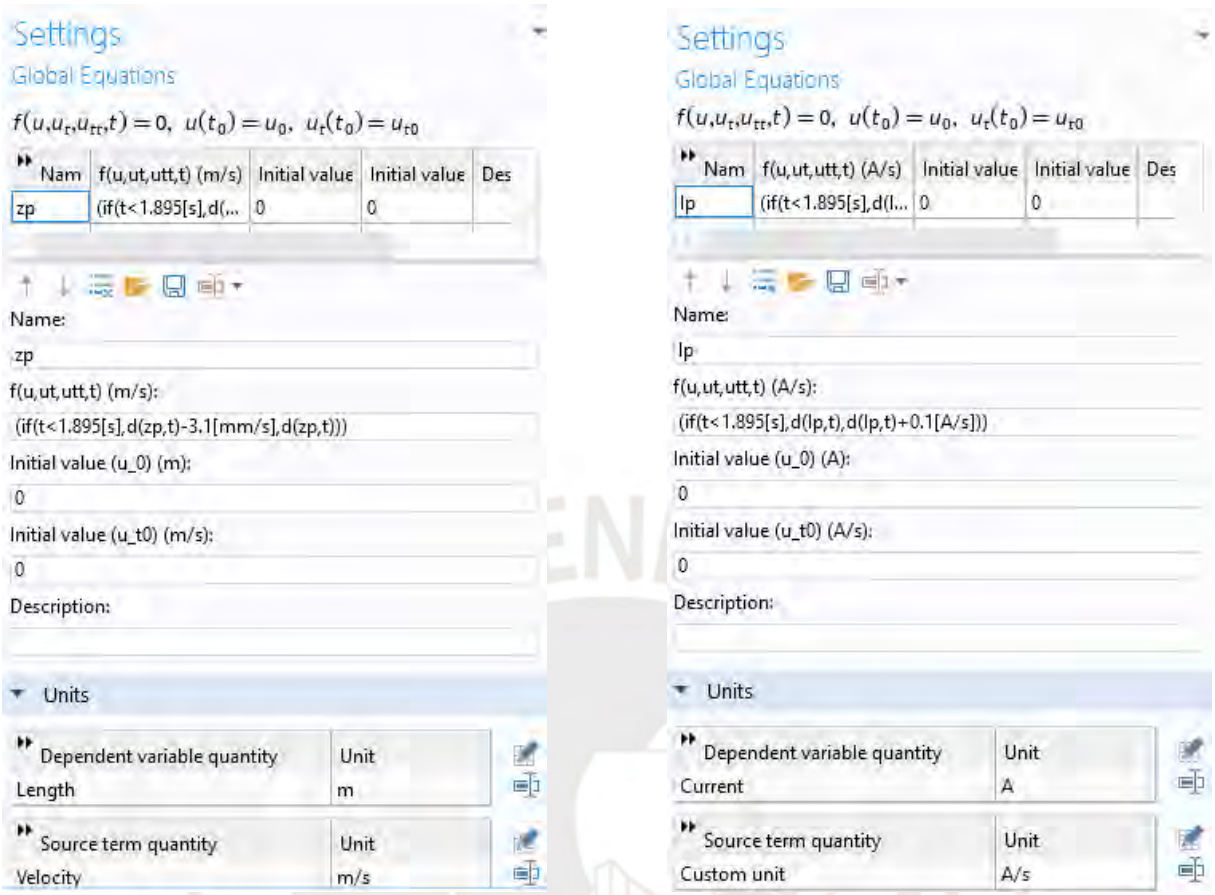

(a) ODEs for position z_p

(b) ODEs for current I_p

Figure 3.28: ODEs implemented for each subprocess in the magnetization process.

Figure 3.29 illustrates the differential equations and simulations required in COMSOL due to the subdivision of processes. It consists of two subfigures: the left side shows the implemented ODEs in the COMSOL Model Builder, while the right side depicts the time-dependent studies (simulations).

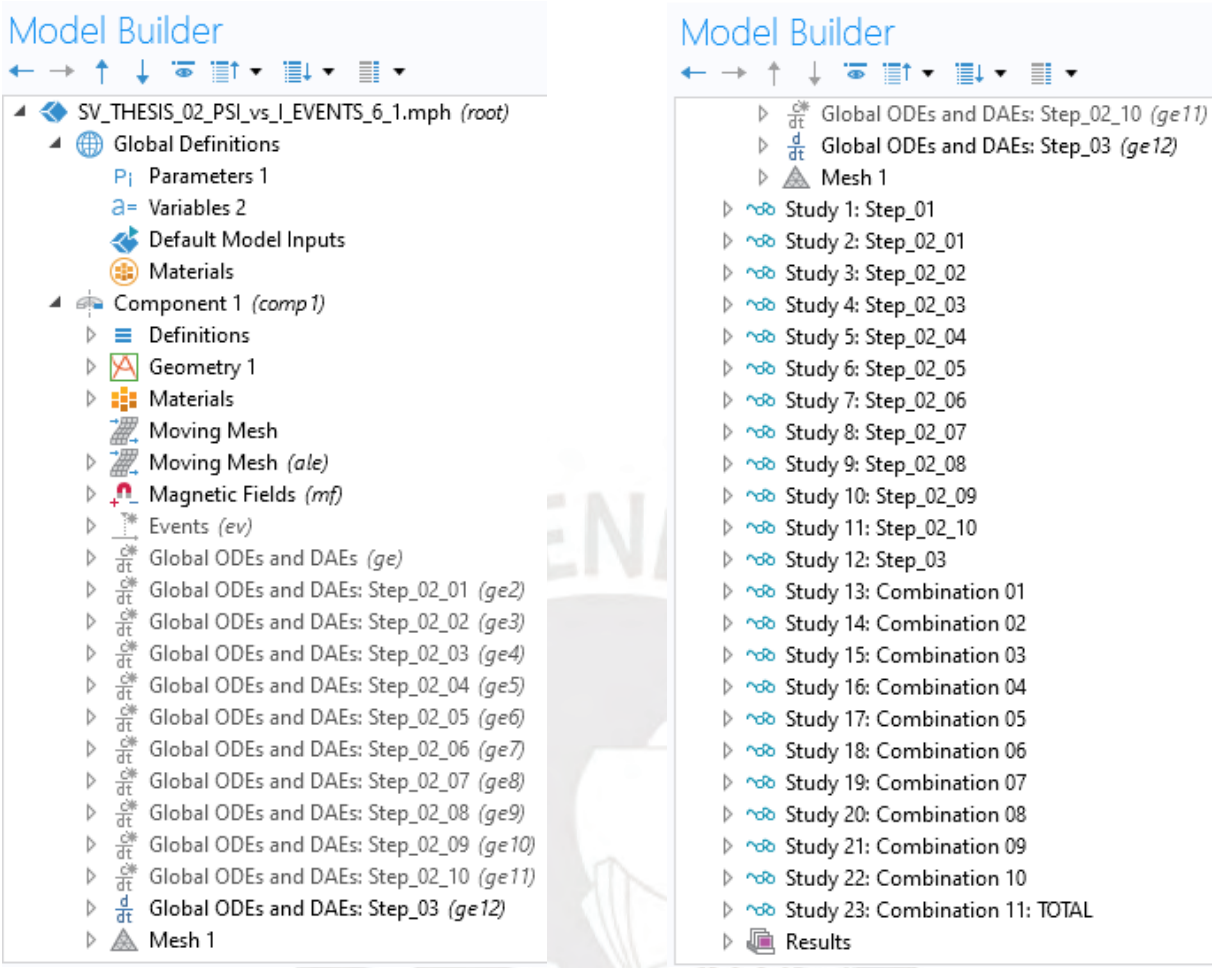

(a) Implemented ODEs in Model Builder

(b) Time-dependent studies in COMSOL

Figure 3.29: Differential equations and simulations required in COMSOL due to the process subdivision.

This process required many hours of work to obtain a Ψ vs I curve. Therefore, this method was no longer considered for the study with variation of mechanical parameters.

However, this study was important to indicate that it is possible to obtain characteristic curves directly from the COMSOL software, but it is not feasible to do so.

3.5 Parameter Studies

To assess potential influences on the RSG 270 series coaxial valve, several parameter studies were conducted. These studies aim to investigate how changes in various mechanical parameters and operational variables could affect the original Ψ vs I characteristic curve and identify potential coil failures. Each study was conducted systematically to evaluate the following variables:

1. **Air Gap:** The initial air gap between the plunger and the core at the start of the actuation cycle, reflecting the coil's condition and potential issues such as material deposits on the valve's 4.2 seal (see Table 2.1) or wear.
2. **Stroke Length:** The distance traveled by the plunger during actuation, impacting the air gap and potentially affecting operational performance.
3. **Friction Force:** The resistance encountered by the plunger due to frictional forces, affecting the smooth operation of the valve.
4. **Return Spring Stiffness:** The initial stiffness of the return spring, affecting the force required to reset the valve.
5. **Coil Temperature:** Variations in the internal temperature of the coil, influencing coil resistance and the magnetic core's properties.

Simulations using MATLAB will observe how these parameters affect the valve's behavior. The data exported from COMSOL includes position x, current I, magnetic force F_z, and concatenated flux Ψ, all dependent on x and I (as seen in Section 2.1.2). The dependence of F_z and Ψ on x and I is illustrated in Figure 3.30.

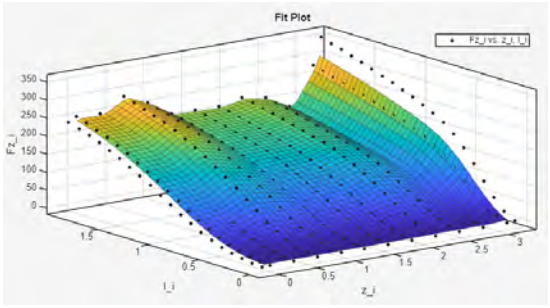

(a) Relationship of magnetic force F_z with respect to z and I

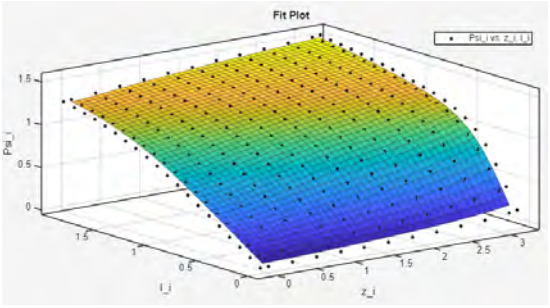

(b) Relationship of concatenated magnetic flux Ψ with respect to z and I

Figure 3.30: Dependence of F_z and Ψ on z and I

The following subsections will detail each parameter study, outlining the methodology (Falling off, Magnetization, Attraction) used to generate characteristic curves (Section 3.4.3) and providing insights into their potential impact on the valve's operational characteristics.

3.5.1 Air Gap

The simulation for the "air gap" parameter is conducted with the following steps:

- **Variation of Air Gap (Falling off):** The air gap systematically varies from 0 mm to 0.5 mm in 0.05 mm increments, following the vector d_gap defined in the Matlab code.
- **Data Import and Processing (Magnetization):** Required data, including position (z), current (I), concatenated flux (Ψ), and magnetic force (F_z), is imported from `data.txt`.
- **Calculation of Ψ vs I Characteristic Curve (Attraction):** Using interpolation techniques (`griddata`), compute Ψ vs I characteristic curves based on the imported data through three steps:
  - **Step 1:** Initialize and increment current to establish baseline data points.
  - **Step 2:** Increment position (z_p) and adjust current to simulate varying air gap conditions.
  - **Step 3:** Continue incrementing current to ensure comprehensive coverage of the Ψ vs I curve.
- **Visualization and Analysis:** Plot and analyze resulting Ψ vs I curves for different air

gap settings.

3.5.2 Stroke Length

For the "stroke length" parameter, the simulation process involves:

- **Initialization of Initial Positions:** Initially set positions z_{p0} as $z_{p0} = [[0.75 : -0.075 : 0.15][0 : -0.15 : -0.45]]$, covering various displacements of the plunger from the coil's rest position.
- **Data Import and Processing:** Import data from `data.txt`, utilizing vectors to store positions (z), current (I), concatenated flux (Ψ), and magnetic force (F_z).
- **Calculation of the Ψ vs I Characteristic Curve:** Calculate the Ψ vs I characteristic curves using interpolation (`griddata`) with imported data, involving:
  - **Step 1:** Initialize and increment current.
  - **Step 2:** Increment position z_p and adjust current.
  - **Step 3:** Continue incrementing current to complete the curve.
- **Visualization:** Prepare and analyze Ψ vs I curves for various initial positions (z_{p0}).

3.5.3 Friction Force

To explore the "friction force" parameter, the simulation involves the following steps:

- **Variation of Friction Force:** Systematically vary F_r from 0 N to 71.5 N in specific increments, defined as $[0, 18.6, 20.35, 25.9, 30.2, 35.9, 40.75, 41.5, 45, 46.9, 51.35, 55.05, 60.2, 66.1, 71.5]$ N.
- **Data Import and Processing:** Import position (z), current (I), concatenated flux (Ψ), and magnetic force (F_z) data from `data.txt`.
- **Calculation of Ψ vs I Characteristic Curve:** Utilize interpolation techniques (`griddata`) to compute Ψ vs I curves based on the imported data through the following steps:
  - **Step 1:** Initiate with $I_p = 0.1$ A and $z_p = 0$, iteratively finding I where F_z exceeds

$F_k + F_r$.

- **Step 2:** Increment z_p in 0.1 mm steps up to 3.1 mm, adjusting I iteratively until $F_z = F_k + F_r$.
- **Step 3:** Continue increasing I until 1.4 A to capture comprehensive Ψ values.

- **Visualization and Analysis:** Plot and analyze resulting Ψ vs I curves for different friction force settings.

These friction forces were chosen to compare the results with those of the SmartValve project study [3].

3.5.4 Return Spring Stiffness

Exploring the "return spring stiffness" parameter involves the following steps:

- **Data Import:** Import position (z), current (I), concatenated flux (Ψ), and magnetic force (F_z) data from `data.txt`.
- **Simulation Steps:** MATLAB simulations are conducted in three main steps to derive the Ψ versus I characteristic curve for different spring stiffness values:
  1. **Step 1 - Initial Iteration:** Start with an initial current $I_p = 0.1$ A and position $z_p = 0$, iterating to find I where the magnetic force F_z exceeds the sum of the spring force F_k and friction force F_r.
  2. **Step 2 - Position Incrementation:** Increment the position z_p in 0.1 mm steps up to 3.1 mm, adjusting I iteratively until $F_z = F_k + F_r$.
  3. **Step 3 - Completion of Curve:** Continue increasing I until 1.4 A to capture comprehensive Ψ values across the entire range of spring stiffness.
- **Parameter Variation:** Vary the spring stiffness k in the simulations across the following values: 1.8, 3.6, 5.4, 7.2, and 9.0 N/mm, corresponding to different physical configurations of the return spring.
- **Visualization and Analysis:** Plot and analyze resulting Ψ versus I curves for each spring stiffness setting.

3.5.5 Coil Temperature

This section investigates the influence of coil temperature variations on the Ψ versus I characteristic curve. The experiments were conducted at four different temperatures: $20°$C, $40°$C, $60°$C, and $80°$C. The procedure for the simulation is detailed below:

- **Data Import:** Import position (z), current (I), concatenated flux (Ψ), and magnetic force (F_z) data from corresponding .txt files (`data_T20C`, `data_T40C`, `data_T60C`, `data_T80C`).
- **Simulation Steps:** MATLAB simulations are performed for each temperature to derive the Ψ versus I characteristic curve, following these steps:
  1. **Step 1 - Initial Iteration:** Start with an initial current $I_p = 0.1$ A and position $z_p = 0$, iterating to determine I where the magnetic force F_z exceeds the sum of spring force F_k, friction force F_r, and temperature-dependent magnetic forces.
  2. **Step 2 - Position Incrementation:** Increment the position z_p in 0.1 mm steps up to 3.1 mm, adjusting I iteratively until $F_z = F_k + F_r$ with temperature-dependent adjustments.
  3. **Step 3 - Curve Completion:** Continue increasing I until 1.4 A to capture comprehensive Ψ values across the entire range of coil temperatures.
- **Parameter Variation:** Analyze the resulting Ψ versus I curves for each temperature setting to understand their influence on the electromagnetic behavior of the valve.
- **Visualization and Analysis:** Plot and analyze the Ψ versus I curves for $20°$C, $40°$C, $60°$C, and $80°$C to compare and contrast the effects of temperature on the coil's magnetic properties.

4 Results

4.1 Presentation of 3D Modelling Results

This section presents the results of the 3D modelling of the valve's magnetic circuit using COMSOL Multiphysics. The analysis focuses on the distribution of the Magnetic Flux Density Norm (MFDN) and the magnetic flux lines under different valve positions when the coil is excited with a 24V voltage source.

4.1.1 Magnetic Flux Density Norm (MFDN)

The 3D Magnetic Flux Density Norm (MFDN) was analyzed for both the closed and open valve positions. Figure 4.1 presents the MFDN in 3D views for these two positions:

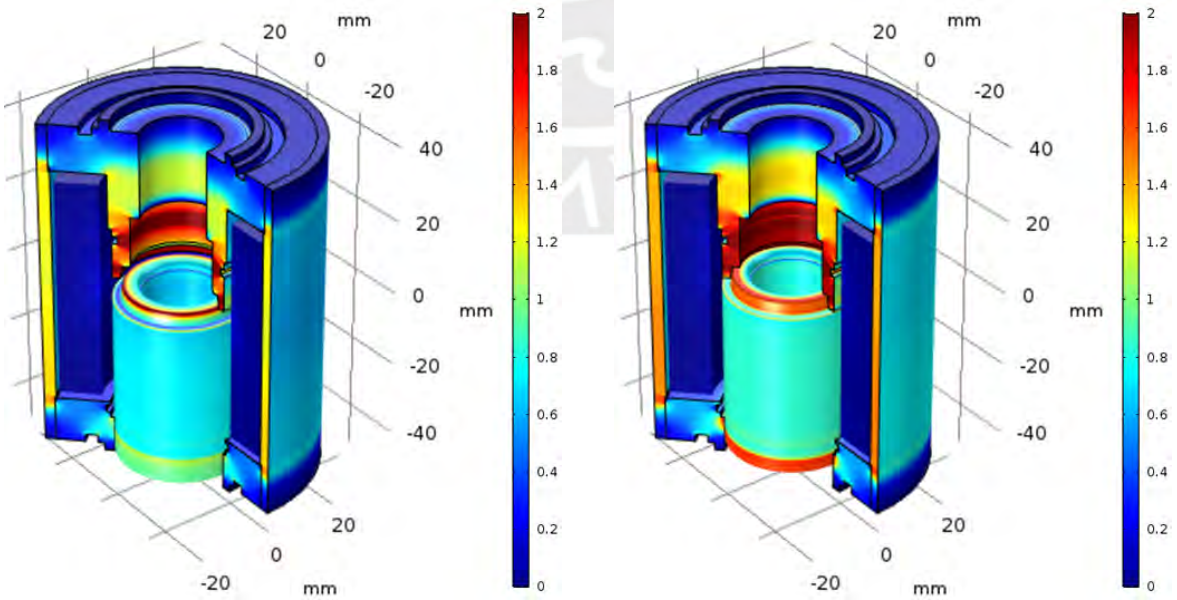

(a) Closed valve position

(b) Open valve position

Figure 4.1: 3D Magnetic Flux Density Norm (Wb) with a 24V excitation.

4.1.2 Magnetic Flux Lines and MFDN in 2D

In addition to the 3D representation, the magnetic flux lines and the MFDN were also evaluated in 2D views. Figure 4.2 shows these distributions for both the closed and open valve positions:

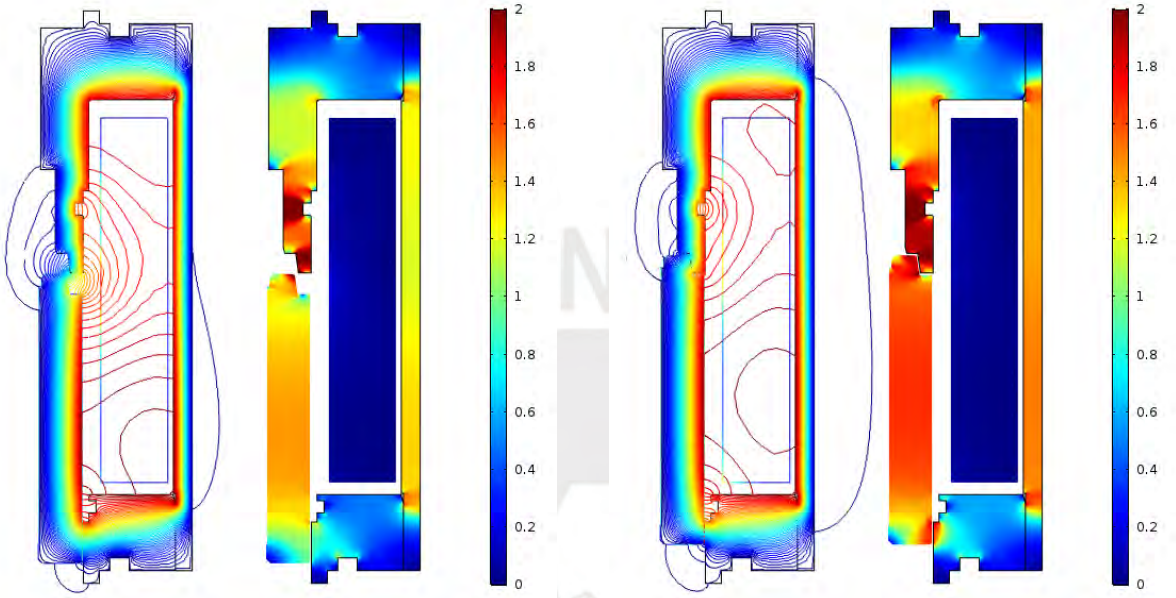

(a) Closed valve position (b) Open valve position

Figure 4.2: Magnetic flux lines and Magnetic Flux Density Norm (MFDN) in 2D with a 24V excitation.

Analysis and Discussion

The results from the 3D and 2D simulations provide significant insights into the behavior of the magnetic circuit under operational conditions. These trends are consistent with the fundamental relationships described in Section 2.1.2, where the magnetic flux Φ is defined as $\Phi = \frac{\mathcal{F}}{\mathcal{R}}$ and the reluctance $\mathcal{R}$ increases proportionally with the air gap length [4]. According to $B = \mu H$, a larger air gap results in a reduction of the magnetic flux density (MFDN) in the circuit.

Closed Valve Position: In the closed valve position, where the air gap is maximum, the MFDN is more widely distributed across the magnetic circuit. The magnetic flux lines are less concentrated, indicating lower magnetic efficiency due to the larger air gap.

Open Valve Position: When the valve is in the open position, where the air gap is minimum, the MFDN is concentrated around the core and coil area, showing stronger magnetic interactions. The magnetic flux lines are denser and follow a clearer path through the magnetic circuit, ensuring more efficient magnetic performance compared to the closed position.

4.2 Presentation of Transverse Forces Calculation Results

This section presents the results of the transverse forces calculation for the valve's magnetic circuit under non-coaxial conditions using COMSOL Multiphysics. The study focuses on the impact of plunger inclination due to seal deformation, which introduces significant transverse forces.

4.2.1 Magnetic Flux Density Norm (MFDN)

The 3D Magnetic Flux Density Norm (MFDN) was analyzed for the inclined plunger geometry. Figure 4.3 presents the MFDN in 3D and 2D views:

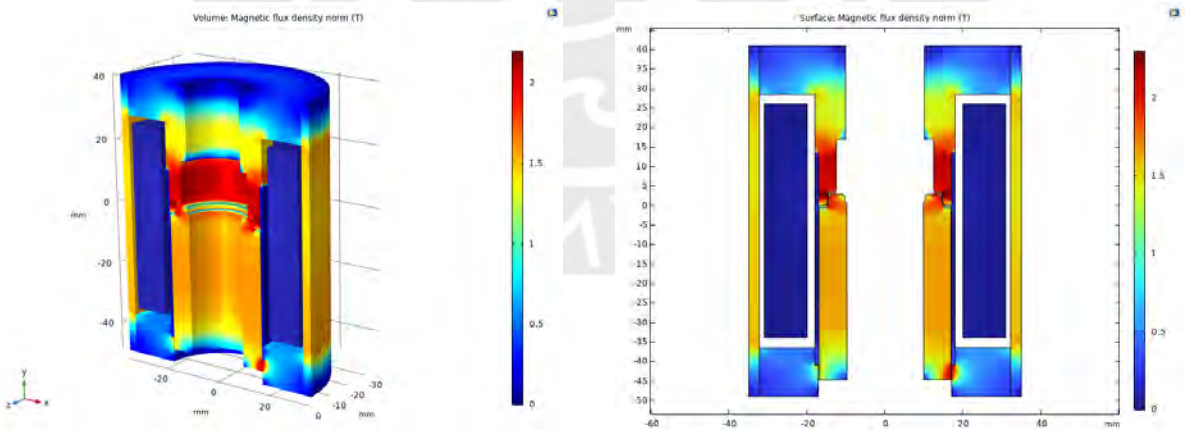

(a) 3D Magnetic Flux Density Norm (MFDN) (b) 2D Magnetic Flux Density Norm (MFDN)

Figure 4.3: Magnetic Flux Density Norm (MFDN) with an inclined plunger.

As shown in the figures, the MFDN is more intense in the lower right part of the plunger due to its inclination. This inclination breaks the symmetry of the MFDN with respect to the yz-plane.

4.2.2 Transverse Forces Calculation

The transverse forces acting on the inclined plunger were calculated by integrating the magnetic stress tensor over the plunger's surface. The simulation results for the half-geometry model yielded the following force components in the COMSOL coordinate system: $F_x = 47.2\,\mathrm{N}$, $F_y = 119.4\,\mathrm{N}$, $F_z = -220.3\,\mathrm{N}$.

Given the system's symmetry with respect to the xy-plane, the resulting forces for the complete valve are:

$$F_x = 94.5\,\mathrm{N}, \quad F_y = 238.8\,\mathrm{N}, \quad F_z = 0\,\mathrm{N}$$

These force components were obtained using a 3D stationary magnetic fields simulation in COMSOL Multiphysics, with the coil excited at 24 V DC, a maximum mesh element size of 1.5 mm in the plunger region, and a magnetic material assignment corresponding to 9SMn28k steel with its measured B–H curve. The magnetic forces were computed via integration of the Maxwell stress tensor over the plunger surface.

Analysis and Discussion

The results from the simulations provide significant insights into the behavior of the valve's magnetic circuit under non-coaxial conditions.

Simulation Challenges: The initial simulations of the complete 3D geometry took more than 12 hours and often ended in errors due to computational singularities. Numerous attempts were made to modify the meshing parameters to achieve a balance between computational effort and accuracy. Finally, a meshing configuration, working with the half of the geometry, was obtained that completed the simulation in approximately 4 hours without errors.

Inclined Plunger Analysis: In the inclined plunger position, the MFDN distribution shows higher intensity in the lower right region, indicating stronger magnetic interactions in this area. The lack of symmetry in the MFDN due to the plunger's inclination results in significant transverse forces acting on the plunger.

Future Work: Due to the extensive computational effort required and the challenges encountered, further simulations varying the plunger position were not conducted. Additionally, another potential misalignment case involves the radial displacement of the plunger parallel to its axis. However, this analysis could not be carried out and remains a proposal for future research.

4.3 Results of 2D Modelling and Transient Simulations

The results from the 2D modelling and transient simulations provide valuable insights into the electromagnetic behavior and transient response of the electromagnetic fluid valve under various conditions. This section presents the findings, emphasizing the complexity and extensive computational effort involved.

4.3.1 Characteristic Curve Ψ vs I

The primary outcome of the 2D simulations was the characteristic curve Ψ vs I, which is crucial for understanding the magnetic flux linkage as a function of the excitation current. The curve was obtained through a series of transient simulations in COMSOL Multiphysics, where the plunger position and excitation current were varied systematically. Figure 4.4 shows the resulting characteristic curve.

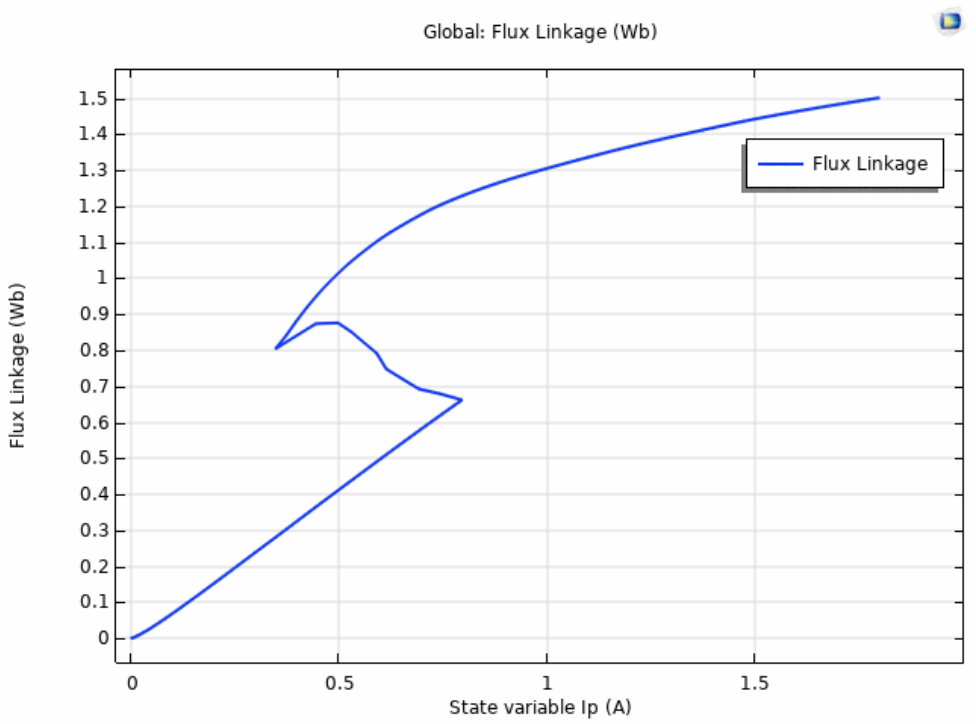

Figure 4.4: Characteristic curve Ψ vs I obtained from transient simulations in COMSOL.

This curve illustrates the relationship between the magnetic flux linkage and the excitation current, reflecting the dynamic response of the valve's magnetic circuit. The complexity of this process is underscored by the fact that a total of 23 simulations were conducted to derive this curve, as illustrated in Figure 3.29 in the previous section.

These results were obtained following the procedure described in Section 3.4.3, where the dynamic simulations were configured to capture the magnetic flux linkage and current during valve actuation. The coil was driven by a programmed current source $I(t)$ (not a fixed voltage), sweeping the operating range with a ramp/hold profile. For each excitation segment, $\Psi(t) = N\,\Phi(t)$ and $I(t)$ were exported and synchronized with the plunger stroke. The model included nonlinear $B{-}H$ characteristics for the ferromagnetic parts, and the mesh and time-step settings were those validated in Section 3.2.3.

The shape of the $\Psi{-}I$ curve reflects the combined effects of air-gap variation and magnetic saturation. At low currents and with a relatively large air gap, Ψ increases nearly linearly with I because the air-gap reluctance dominates. As the plunger advances and the effective air gap decreases, the slope $d\Psi/dI$ increases. At higher currents, the ferromagnetic regions approach saturation (i.e., the effective permeability decreases), which reduces $d\Psi/dI$ and produces the

characteristic flattening at the upper end of the curve (see Section 2.1.2 and [4]).

4.3.2 Challenges and Computational Effort

The process of obtaining the Ψ vs I curve was intricate and time-consuming. Each simulation required careful setup and execution, often taking significant computational resources. The transient simulations involved varying the plunger position and current over time, capturing the dynamic behavior of the valve under different conditions.

Several challenges were encountered during this process:

- **Complexity of Transient Simulations:** The transient nature of the simulations necessitated precise control over the parameters, requiring detailed configuration of the Moving Mesh and Global ODEs and DAEs modules in COMSOL.
- **High Computational Load:** Each simulation was computationally intensive, with some runs taking several hours to complete. The total time spent on these simulations was substantial, highlighting the demanding nature of the study.
- **Segmentation of Processes:** To manage the complexity, the simulations were segmented into manageable steps, with each subprocess requiring specific ODE implementations. This segmentation is shown in Figure 3.29, where differential equations and time-dependent studies were implemented in the COMSOL Model Builder.

Future Work

While the current study provides a comprehensive analysis of the 2D modelling and transient simulations, further research is necessary to explore other aspects of the valve's behavior. Future work could include:

- **3D Simulations:** Extending the analysis to full 3D simulations to capture more detailed spatial variations in the magnetic field and forces.
- **Parameter Variations:** Investigating the effects of different mechanical parameters, such as friction, return spring stiffness, and temperature, on the valve's performance.
- **Optimization Studies:** Conducting optimization studies to identify the best design pa-

rameters for improved performance and efficiency.

4.4 Results of Parameter Studies

This section presents the results of the parameter studies conducted on the RSG 270 series coaxial valve. Each parameter was systematically varied, and the resulting Ψ vs I characteristic curves were analyzed to understand their effects on the valve's performance. The simulations were performed using MATLAB, with data exported from COMSOL, including position x, current I, magnetic force F_z, and concatenated flux Ψ.

4.4.1 Air Gap

The effect of varying the air gap between the plunger and the core on the Ψ vs I characteristic curve was studied. The air gap was varied from 0 mm to 0.5 mm in 0.05 mm increments. Figure 4.5 shows the simulation results.

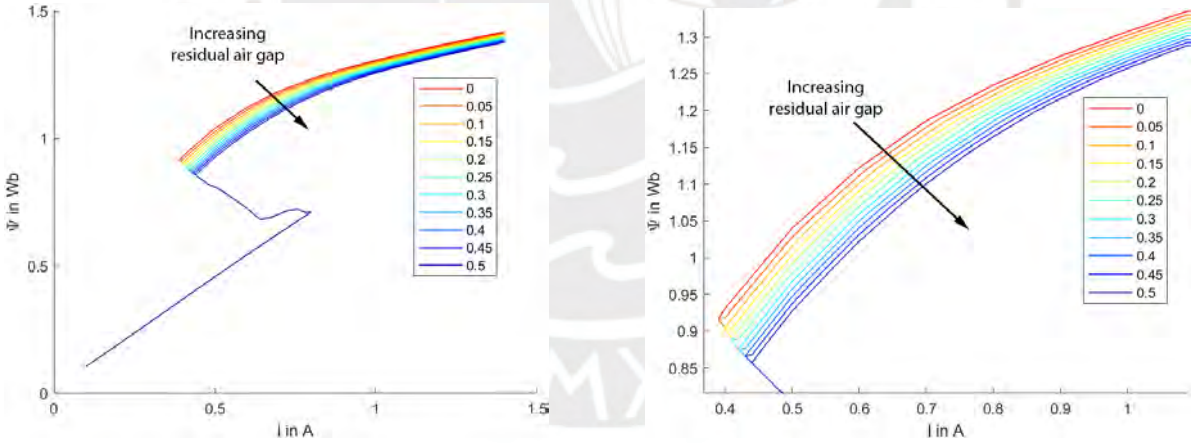

(a) Ψ vs I curve with varying air gap

(b) Detail of the Ψ vs I curve at the beginning of the attraction process

Figure 4.5: Effect of air gap variation on the Ψ vs I characteristic curve

We can observe that the lower part of the curve and the motion process section show consistent behavior across different air gap sizes, suggesting stable performance before and during the attraction phase. In contrast, the upper part of the curve illustrates the impact of increasing residual air gap. With a wider air gap, the curve exhibits a more pronounced descent after

initial stick-slip behavior during armature attraction, attributed to heightened magnetic air gap resistance post-attraction due to the larger residual air gap. This results in a lower magnetic flux density under identical current and magnetic flux conditions. Additionally, deposits may form on the plunger if the valve's dynamic seals allow, potentially increasing friction and exacerbating the effects of increased residual air gap observed in measurement curves.

4.4.2 Stroke Length

The influence of stroke length on the Ψ vs I characteristic curve was investigated by initializing the positions z_{p0} from 0.75 mm to 0.15 mm in 0.075 mm decrements, and from 0 mm to -0.45 mm in 0.15 mm decrements. The simulation results are presented in Figure 4.6.

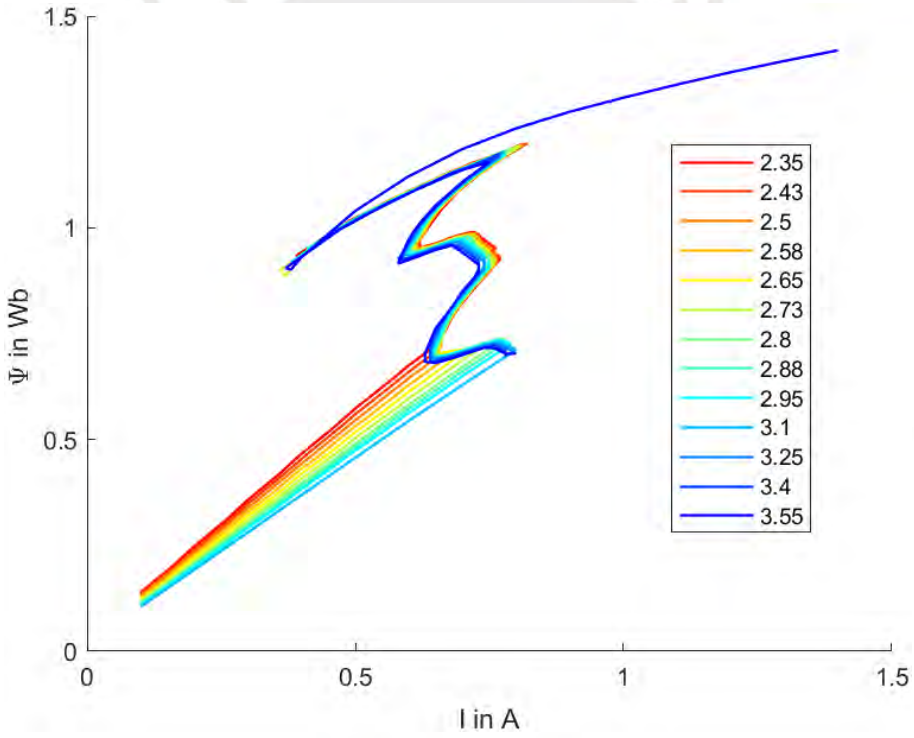

Figure 4.6: Ψ vs I curve for various initial positions

The simulated Ψ vs I characteristic curve reveals significant sensitivity to stroke length variations. As shown in Figure 4.6, increasing stroke length leads to an increase in magnetic air gap resistance R_{mx}, resulting in a corresponding decrease in the slope of the $\Psi(i, \delta)$ curves up to the armature attraction phase. This trend indicates that larger stroke lengths require higher magnetic flux densities to achieve comparable magnetic flux levels due to increased magnetic resistance.

4.4.3 Friction Force

To study the impact of friction force on the Ψ vs I characteristic curve, the friction force was varied from 0 N to 71.5 N in specific increments. The simulation results are depicted in Figure 4.7.

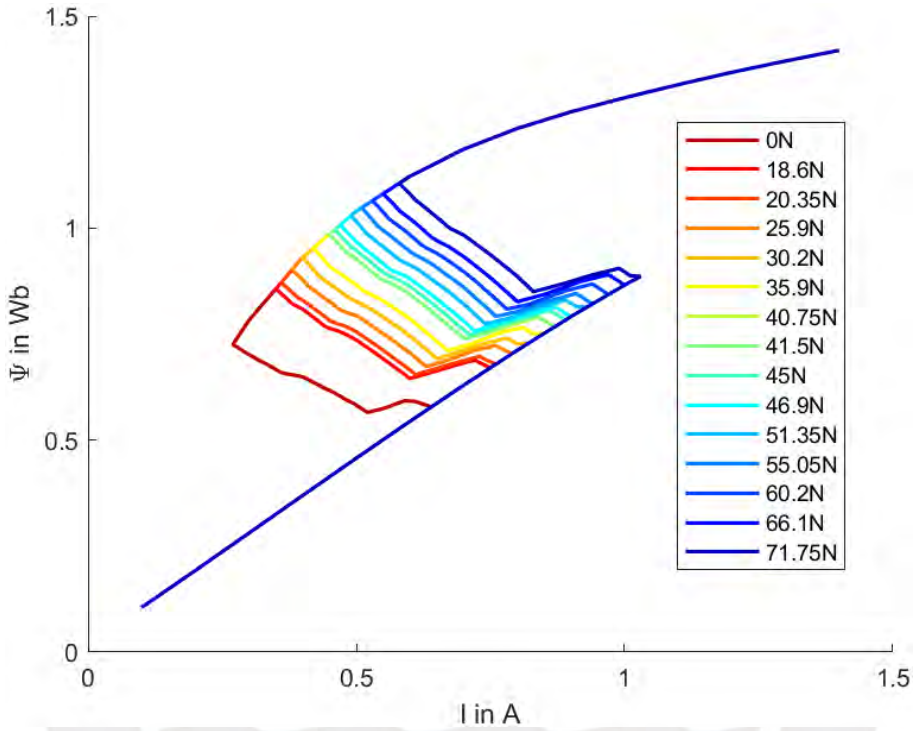

Figure 4.7: Ψ vs I curve with varying friction force

Increasing friction force results in higher opposing forces during armature movement. Consequently, a higher magnetic force is required to attract the armature, which affects the $\Psi(i, \delta)$ curve. This implies that more current is needed before entering the magnetization process.

4.4.4 Return Spring Stiffness

The impact of return spring stiffness on the Ψ vs I characteristic curve was examined by varying the spring stiffness k across different values. Figure 4.8 presents the results of these simulations.

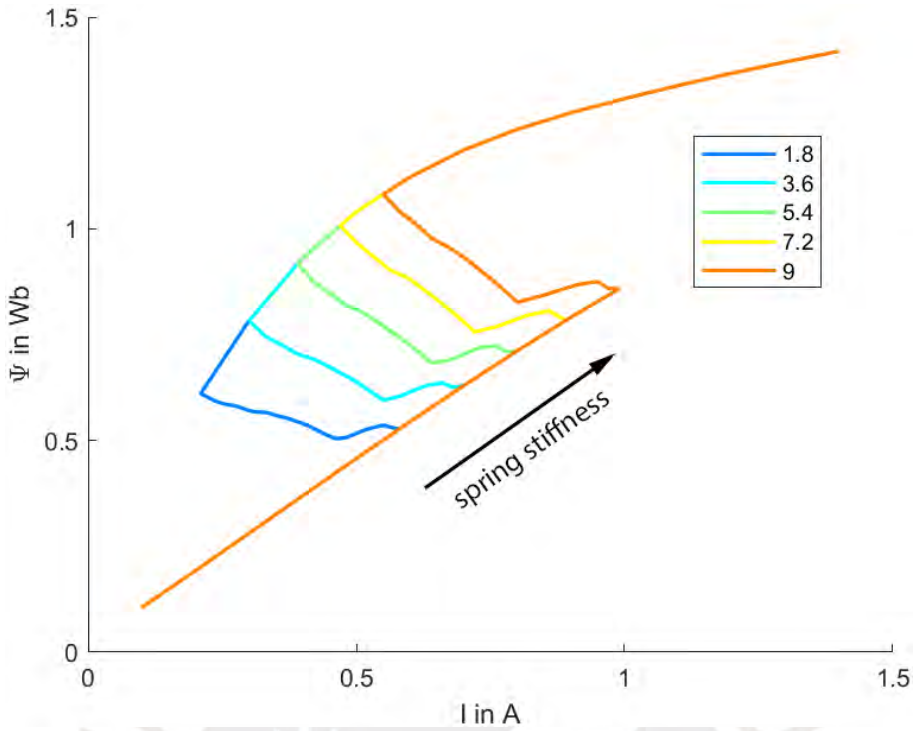

Figure 4.8: Effect of return spring stiffness on the Ψ vs I characteristic curve

It is observed that the behaviour of the curve is similar to that observed with variable friction force. Increasing the spring stiffness necessitates a higher magnetic force to attract the armature, thus requiring more current.

4.4.5 Coil Temperature

The influence of coil temperature on the Ψ vs I characteristic curve was studied at four different temperatures: $20°C$, $40°C$, $60°C$, and $80°C$. The results are shown in Figure 4.9.

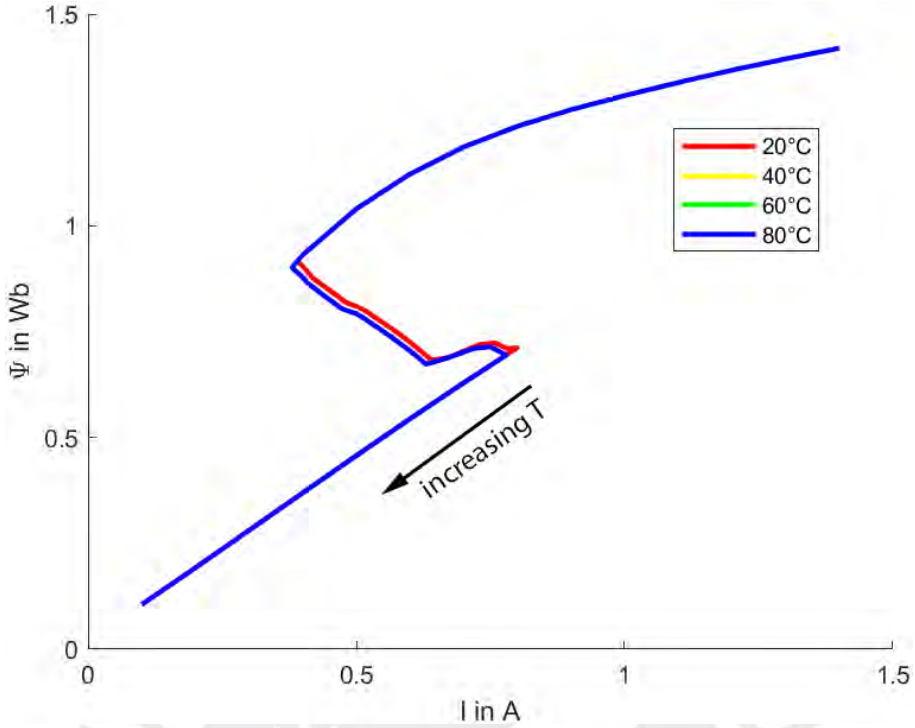

Figure 4.9: Effect of coil temperature on the Ψ vs I characteristic curve

In the curve, it is evident that higher temperatures lead to a quicker transition of the armature into the magnetisation process. Eddy currents, induced by time-varying magnetic fields in the electrically conductive iron of the magnetic circuit, generate opposing magnetic fields that impede the establishment of the desired magnetic flux. With increasing temperature, the electrical resistance of the iron also rises, thereby diminishing the strength of these eddy currents. Consequently, the counteracting magnetic field that impedes magnetic flux accumulation decreases, allowing the magnetic flux to rise more rapidly for a given electrical current and magnetic voltage.

4.4.6 Comparison with SmartValve Project Results

To validate the simulation results, a comparison was made with the findings from the SmartValve project for the parameters of air gap, stroke length, and friction force. Figures 4.10, 4.11, and 4.12 illustrate this comparison.

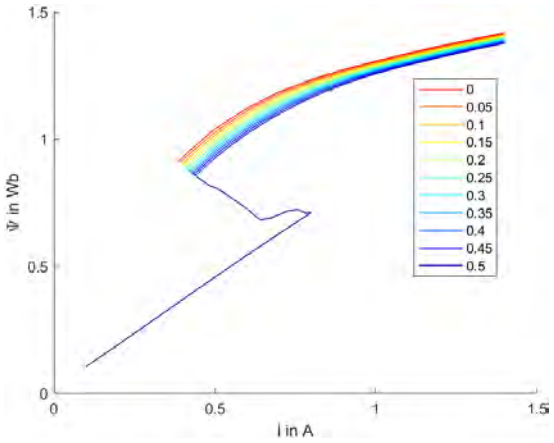

(a) Air gap simulation results

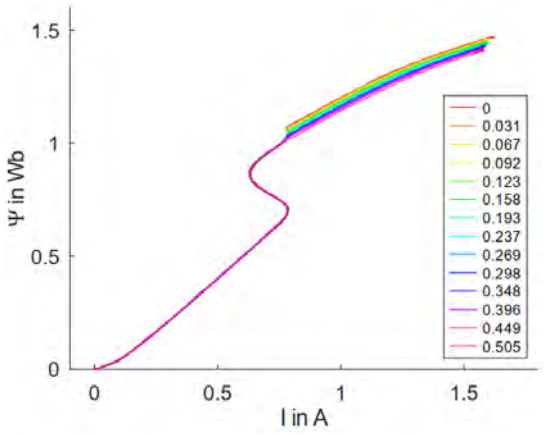

(b) Air gap SmartValve project results [3]

Figure 4.10: Comparison of air gap results

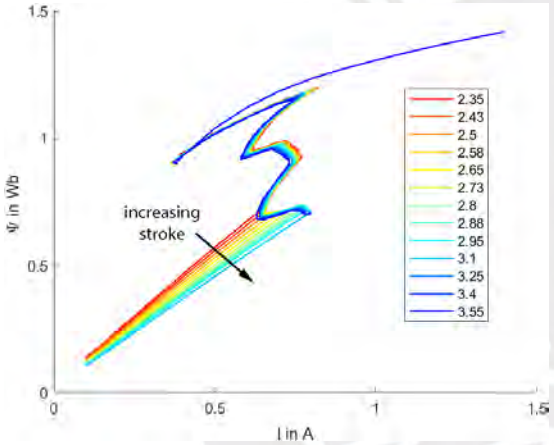

(a) Stroke length simulation results

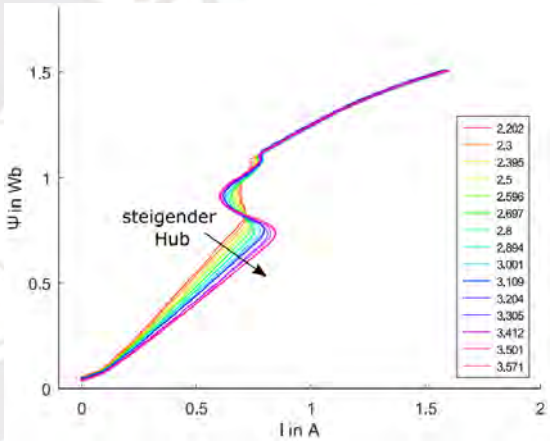

(b) Stroke length SmartValve project results [3]

Figure 4.11: Comparison of stroke length results

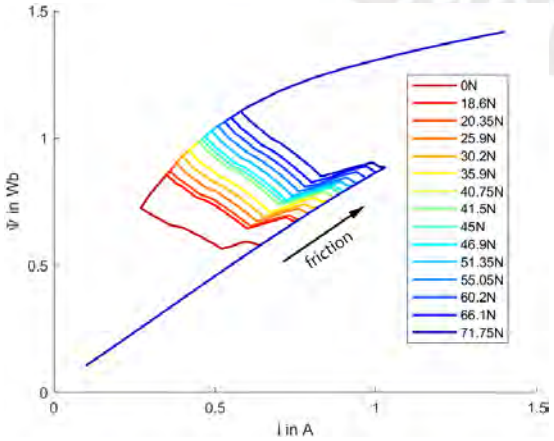

(a) Friction force simulation results

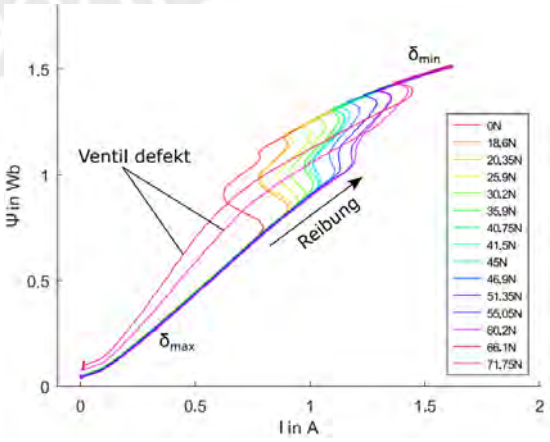

(b) Friction force SmartValve project results [3]

Figure 4.12: Comparison of friction force results

These comparisons demonstrate the consistency of the simulation results with the experimental findings of the SmartValve project, validating the reliability and accuracy of the parameter studies conducted in this research. The differences observed in the curve shapes are mainly attributed to variations in test conditions and to simplifications made in the numerical model, such as neglecting certain parasitic effects present in the real system, minor deviations in material permeability from measured values, and mechanical tolerances not represented in the simulated geometry. These factors explain the local discrepancies without affecting the overall agreement between simulation and experiment.

4.5 Sensitivity Analysis and Its Impact

Sensitivity analysis was conducted to understand the impact of varying key parameters on the performance of the RSG 270 series coaxial valve. The parameters studied were the residual air gap ($\delta_{\min}$), stroke length (x_0), and friction force (F_r). This section presents the analysis of the sensitivity of the system to these parameters, using the results obtained from the simulations described previously.

The measured magnetization curves in Figures 4.5-4.7 show that the different mechanical system parameters influence different areas of the curve. Conversely, suitable magnetic parameters can be used to infer the cause. Suitable detection parameters are the average slope in the initial range (m_{vAn}), the concatenated flux (Ψ_{diff}) in the upper range (the flux is chosen so that the current is above the pick-up current and below the smallest temperature-dependent maximum current, here 1 A), and the pick-up flux (Ψ_{start}) at the pick-up current, see Figure 4.13.

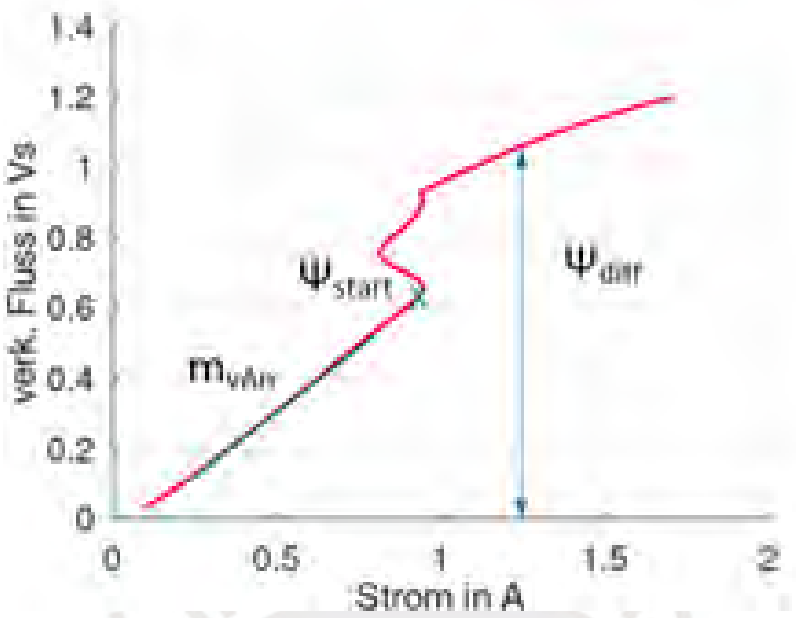

Figure 4.13: Characteristic features of the magnetization curve for wear detection [3]

4.5.1 Impact of Residual Air Gap on Flux Difference

The residual air gap ($\delta_{\min}$) between the plunger and the core was varied from 0 mm to 0.5 mm. The difference in concatenated flux Ψ at a specific operating point (index 163) was recorded for each air gap value. The linear relationship between the residual air gap and the flux difference was determined using a polynomial fit. The results are shown in Figure 4.14.

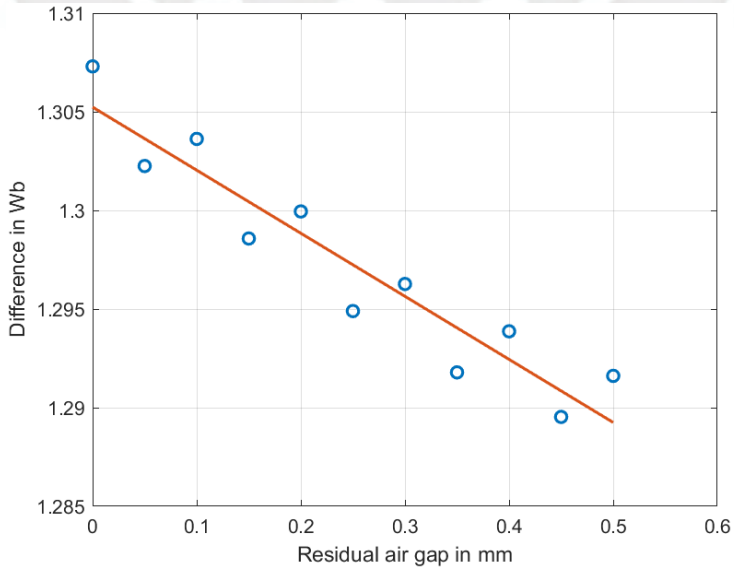

Figure 4.14: Sensitivity of concatenated flux Ψ to residual air gap $\delta_{\min}$

The plot in Figure 4.14 indicates a linear decrease in the concatenated flux as the air gap increases. This relationship can be expressed as:

$$\Psi_{\text{diff}} = -0.0320 \frac{\text{Wb}}{\text{mm}} \cdot \delta_{\text{min}} + 1.3052\,\text{Wb} \tag{4.1}$$

4.5.2 Impact of Stroke Length on Average Slope

The stroke length (x_0) was varied, and the average slope $d\Psi/dI$ of the Ψ vs I curve was calculated for different initial positions z_{p0}. The relationship between the stroke length and the average slope was analyzed using a linear regression model. The results are shown in Figure 4.15.

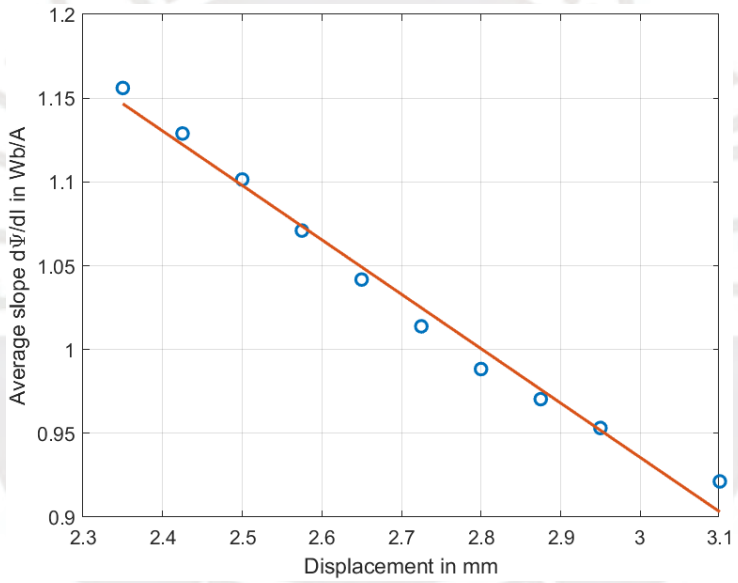

Figure 4.15: Sensitivity of average slope $d\Psi/dI$ to stroke length x_0

Figure 4.15 demonstrates a linear relationship between the stroke length and the average slope of the Ψ vs I curve. This can be expressed as:

$$m_{vAn} = -0.3247 \frac{\text{Wb}}{\text{A} \cdot \text{mm}} \cdot x_0 + 1.9097 \frac{\text{Wb}}{\text{A}} \tag{4.2}$$

4.5.3 Impact of Friction Force on Starting Flux

The impact of varying friction force on the starting flux Ψ_{start} was studied. The friction force was varied from 0 N to 71.5 N, and the starting flux was recorded. A linear regression model was used to describe the relationship between the friction force and the starting flux. The results are presented in Figure 4.16.

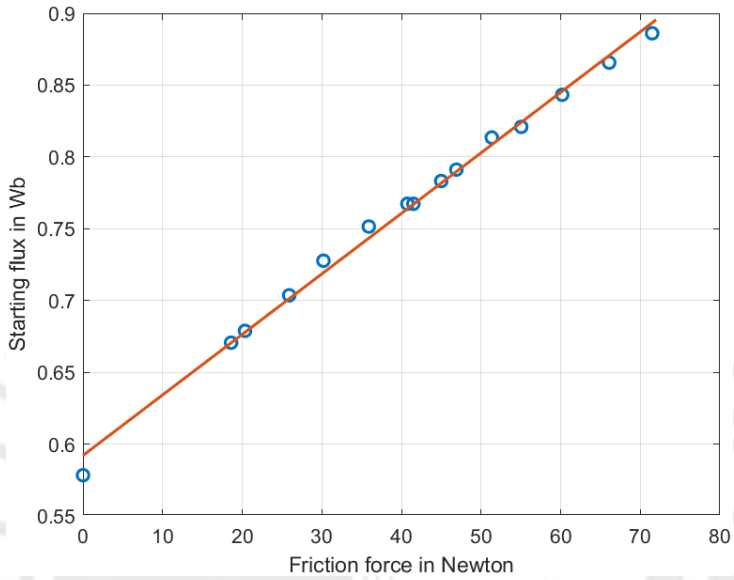

Figure 4.16: Sensitivity of starting flux Ψ_{start} to friction force

The plot in Figure 4.16 illustrates a linear decrease in the starting flux with increasing friction force. This relationship is given by:

$$\Psi_{\text{start}} = 0.0042 \frac{\text{Wb}}{\text{N}} \cdot \text{Fr} + 0.5921\,\text{Wb} \tag{4.3}$$

Discussion

The sensitivity analysis reveals that the performance of the RSG 270 series coaxial valve is significantly influenced by the studied parameters. The linear relationships observed in the sensitivity plots indicate predictable changes in performance metrics with varying parameters. This information is crucial for the design and optimization of the valve, ensuring reliable operation under different conditions. The linear models derived from the sensitivity analysis can be used to predict the impact of parameter variations and guide the design process to achieve desired

performance characteristics. The consistency of these linear relationships with those observed in the SmartValve project further validates the robustness of the analysis.

To further validate our findings, we compare our results with those obtained in the SmartValve project. The following figures depict the dependencies observed in our analysis alongside corresponding results from the SmartValve project:

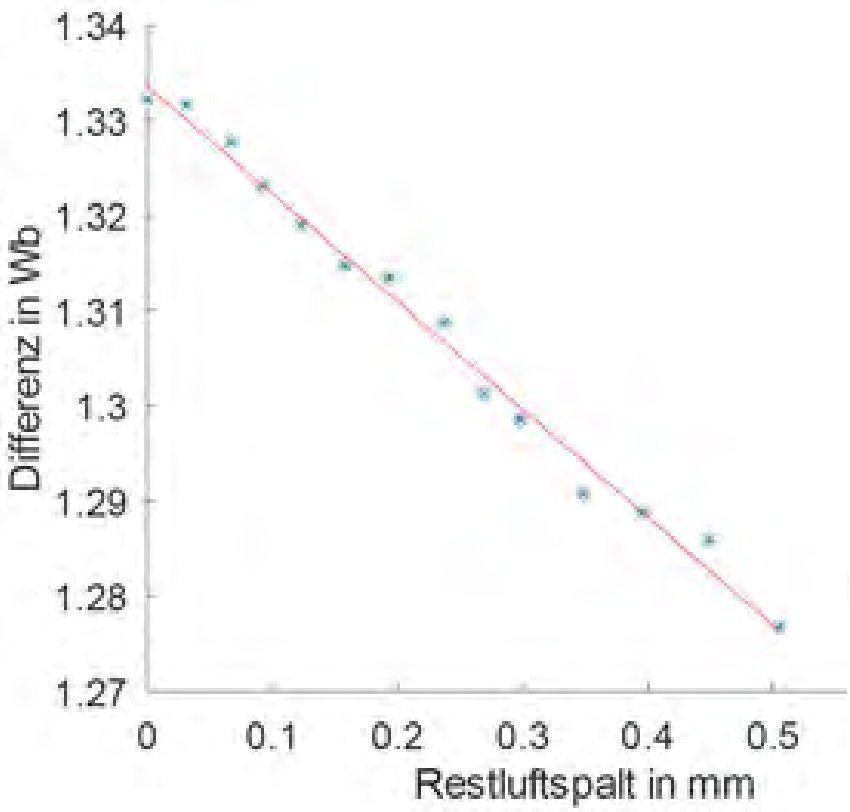

Figure 4.17: Dependency of concatenated flux Ψ_{diff} at current $I = 1$ A on residual air gap $\delta_{\min}$ (pulled state) [3]

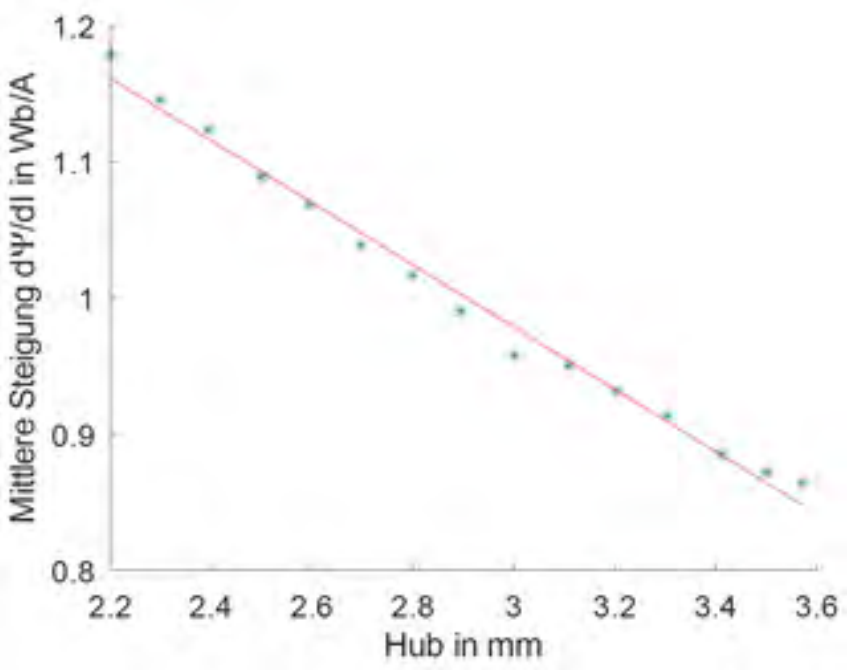

Figure 4.18: Dependency of initial slope m_{vAn} on stroke length x_0 (End stop) [3]

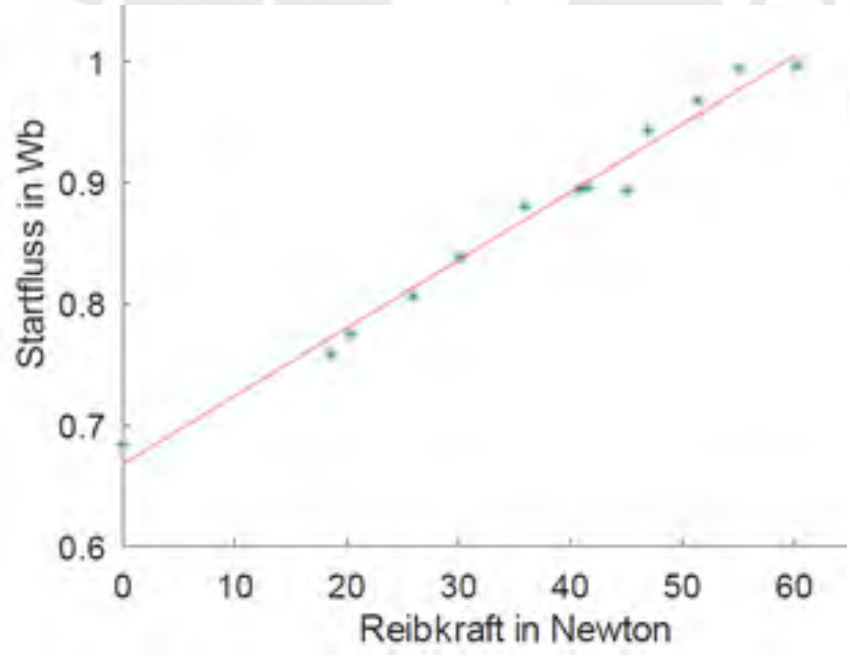

Figure 4.19: Dependency of starting flux Ψ_{start} at motion start on friction force F_r [3]

5 Conclusions

In this thesis, a comprehensive multi-domain model of an electromagnetic fluid valve was developed using COMSOL Multiphysics. The study focused on understanding the complex interactions between electrical excitation, magnetic fields, and mechanical dynamics within the valve's magnetic circuit. The following conclusions can be drawn from the research:

The 3D modelling of the valve's magnetic circuit provided valuable insights into the distribution of magnetic flux density norm (MFN) and magnetic flux lines under different operational conditions. The simulations highlighted the importance of valve position (open versus closed) in influencing magnetic efficiency and flux distribution. Specifically, the open valve position showed concentrated MFN around the core and coil area, indicating more efficient magnetic interactions compared to the closed position.

Transverse force calculations for non-coaxial conditions revealed significant forces acting on the inclined plunger due to seal deformation. The analysis underscored the impact of plunger inclination on MFN distribution and transverse forces, demonstrating the non-symmetrical nature of magnetic interactions in such scenarios.

The 2D modelling and transient simulations provided further insights into the valve's dynamic response to electrical excitation and mechanical parameters. The characteristic curve Ψ vs I obtained from transient simulations illustrated the complex relationship between magnetic flux linkage and excitation current, emphasising the dynamic nature of the valve's magnetic circuit.

Parameter studies conducted on the RSG 270 series coaxial valve highlighted the sensitivity of performance metrics (such as flux linkage and force characteristics) to variations in mechanical parameters (air gap, stroke length, friction force, return spring stiffness, and coil temperature). The linear relationships derived from sensitivity analyses facilitated predictions of performance under different operating conditions, supporting the design and optimisation of the valve for

enhanced efficiency and reliability.

Comparison of simulation results with measurements from the SmartValve project validated the accuracy and reliability of the developed model. Consistent findings between simulation and experimental data confirmed the robustness of the parameter studies and sensitivity analyses conducted in this research.

In this thesis, the term optimisation refers to improvements in the computational model and workflow rather than to a design optimisation of the physical valve. The adopted criteria were: (i) preserve the accuracy of key outputs (e.g., axial force and flux linkage) within the tolerances established by the mesh and time–step independence studies; (ii) eliminate non-critical geometric features (e.g., sub-millimetre air gaps and unnecessary detail) that lead to meshing difficulties or magnetic singularities; and (iii) reduce wall-clock time per simulation while maintaining the functional dimensions of the RSG 270 valve and the aforementioned accuracy targets. Applying these criteria to the simplified geometry (Section 3.2.2) yielded a representative reduction of 47% in simulation time and prevented numerical failures, without degrading solution fidelity, as supported by the convergence analyses in Section 3.2.3 and the subsequent validation in Chapter 4.

Beyond these contributions, the findings suggest practical optimisation strategies for future work: selecting a mesh size that meets the error tolerance with minimal computational cost (Section 3.2.3); prioritising high-fidelity modelling effort on the most influential parameters identified by the sensitivity study (Chapter 4); and leveraging reduced-order or surrogate models to accelerate extensive parametric exploration once accuracy bounds are verified. These strategies, grounded in the present results, provide a reproducible pathway to robust and efficient numerical studies of electromagnetic valves.

Overall, this thesis contributes to the understanding and optimisation of electromagnetic fluid valves through advanced modelling techniques and sensitivity analysis. The findings provide a foundation for further research in improving valve performance, reducing engineering times, and advancing electromagnetic fluid valve technology for various industrial applications.

Bibliography

[1] Frank Lamb. *Industrial Automation: Hands-On*. McGraw-Hill Education, New York, 1st edition edition, 2013.

[2] W. Bolton. *Mechatronics: Electronic Control Systems in Mechanical and Electrical Engineering*. Pearson Higher Education, 7 edition, dec 2018.

[3] Tom Ströhla, Oliver Radler, Marian Ohl, and Thomas Sattel. Smartvalve: Intelligentes condition monitoring für elektromagnetische ventile. *TU Ilmenau, Fachgebiet Mechatronik*, 2023.

[4] Eberhard Kallenbach, Rüdiger Eick, Tom Ströhla, Karsten Feindt, Matthias Kallenbach, and Oliver Radler. *Elektromagnete: Grundlagen, Berechnung, Entwurf und Anwendung*. Springer Vieweg, 5 edition, 2018.

[5] Sakahisa Nagai, Takahiro Nozaki, and Atsuo Kawamura. Real-time sensorless estimation of position and force for solenoid actuators. *IEEJ Journal of Industry Applications*, 5:1–2, 03 2016.

[6] F. Xie, R. Zhou, D. Wang, J. Ke, X. Guo, and V. X. Nguyen. Simulation study on static and dynamic characteristics of electromagnet for electro-hydraulic proportional valve used in shock absorber. *IEEE Access*, 8:41870–41881, 2020.

[7] L. Nagy, T. Szabó, and E. Jakab. A novel method for measuring inductance of an electromagnetic actuator. In *Proceedings of the 13th International Carpathian Control Conference (ICCC)*, pages 511–514, 2012.

[8] Seungjin Yoo, Joon Jung, Jai-Kyung Lee, Sang Shin, and Dal Jang. A convolutional autoencoder based fault diagnosis method for a hydraulic solenoid valve considering unknown faults. *Sensors*, 23:7249, 2023.

[9] David Jiles. *Introduction to Magnetism and Magnetic Materials*. CRC Press, 3 edition, 2015.

[10] M. Yang et al. Magnetic properties measurement and analysis of high frequency core materials considering temperature effect. *IEEE Transactions on Applied Superconductivity*, 30(4):1–5, June 2020.

[11] W. Xu, N. Duan, S. Wang, Y. Guo, and J. Zhu. Modeling and measurement of magnetic hysteresis of soft magnetic composite materials under different magnetizations. *IEEE Transactions on Industrial Electronics*, 64(3):2459–2467, March 2017.

[12] Hartmut Janocha, editor. *Actuators: Basics and Applications*. Springer, Berlin, Heidelberg, 2004 edition, 2004.

[13] TU Ilmenau FG Mechatronik. Smarte direktgesteuerte industrieschaltventile. Technical report, 2021. (siehe S. 9–12, 15 f., 38 f.).

[14] Z. Peng, L. Chen, L. Wei, W. Gao, Q. Yu, and C. Ai. Analysis and identification of a dynamic model for proportional solenoid. *IEEE Access*, 9:92651–92660, 2021.

[15] X. Xiao-qing and Q. Long. A novel analysis method for proportional solenoid magnetic circuit. In *Proceedings of 2011 International Conference on Fluid Power and Mechatronics*, pages 314–318, Beijing, China, 2011.

[16] Jiang Guo, Linguang Li, Pu Qin, Jinghao Wang, Chao Ni, Xu Zhu, Dingyao Lu, and Jiwu Tang. Optimization design of magnetic isolation ring position in ac solenoid valves for dynamic response performances. *Micromachines*, 13(7):1065, 2022.

[17] Masruki Kabib, I Made, Londen Batan, Bambang Pramujati, and Agus Sigit. Modelling and simulation analysis of solenoid valve for spring constant influence to dynamic response. *Journal of Engineering and Applied Sciences*, 11:2790, 2016.

[18] Ibrahim Assi. Electromagnet design for a time varying magnetic flux leakage system. Master's thesis, University of Toronto, 2019.

[19] F. Meng, H. Zhang, D. Cao, and H. Chen. System modeling, coupling analysis, and experimental validation of a proportional pressure valve with pulsewidth modulation control. *IEEE/ASME Transactions on Mechatronics*, 21(3):1742–1753, June 2016.

[20] Mengkun Lu, Zhifang Yuan, and Xianglie Yi. Magnetic field analysis and thrust verification of solenoid actuator based on subdomain method. *Machines*, 12:354, 2024.

[21] Zichen Zhang. Optimised design for high-speed solenoid valves with dual coils. *Journal of Physics: Conference Series*, 2557:012036, 2023.

[22] Nirmal Paudel. Part 1: How to model a linear electromagnetic plunger. https://www.comsol.com/blogs/part-1-how-to-model-a-linear-electromagnetic-plunger, June 2016. Accessed: 2024-07-10.

[23] Nirmal Paudel. Part 2: Model a linear electromagnetic plunger with a blocker. https://www.comsol.com/blogs/part-2-model-a-linear-electromagnetic-plunger-with-a-blocker, June 2016. Accessed: 2024-07-10.